3-Metalla-1,2-dioxolanes and Their Reactivity

Monique Krom,[a] Theo P. J. Peters,[a] Ruud G. E. Coumans,[a] Timo J. J. Sciarone,[a]
Johan Hoogboom,[a] Sandra I. ter Beek,[a] Paul P. J. Schlebos,[a] Jan M. M. Smits,[a]
René de Gelder,[a] and Anton W. Gal*[a]

Keywords: Formylmethyl complexes / Metallacycles / N ligands / Oxygenations / Rhodium

The ethene complexes $[M^{I}(CH_2CH_2)]^+$ (M = Ir, Rh) can be oxygenated by molecular oxygen or air in the solid state, to form isolable unsubstituted 3-metalla-1,2-dioxolanes $[M^{III}(CH_2CH_2OO\text{-}\kappa^2C^1,O^2)]^+$. Such selectivity could not be achieved in solution. The stereoselectivity of the oxygenation process is highly dependent on the ligand, the metal and the counterion used. Oxygenation of $[(tpa)M(CH_2CH_2)]PF_6$ {tpa = tri(2-pyridylmethyl)amine; **4**PF_6, **7**PF_6} results in the formation of two isomeric 3-metalladioxolanes, whereas oxygenation of $[(tpa)M(CH_2CH_2)]BPh_4$ (**4**BPh_4, **7**BPh_4) only yields one isomer. Furthermore, oxygenation of $[(Metpa)Rh(CH_2CH_2)]PF_6$ {**14**PF_6, Metpa = [(6-methyl-2-pyridyl)methyl]bis(2-pyridylmethyl)amine} proved to be much slower than that of $[(tpa)Rh(CH_2CH_2)]PF_6$ (**7**PF_6). The *solid* propene complex $[(tpa)Rh(CH_2CHCH_3)]BPh_4$ (**23**BPh_4) loses propene on reaction with molecular oxygen, and selectively forms the peroxo complex $[(tpa)Rh(\eta^2\text{-}O_2)]BPh_4$ (**24**BPh_4). The obtained 3-metalla-1,2-dioxolanes rearrange, both in the solid state and in solution, to formylmethyl hydroxy complexes on exposure to photons or protons. The isomeric 3-rhoda-1,2-dioxolanes $[(tpa)Rh(CH_2CH_2OO\text{-}\kappa^2C^1,O^2)]^+$ **8a**$^+$ and **8b**$^+$ differ in reactivity. On exposure of a solution of **8a**PF_6/**8b**PF_6 to glass-filtered daylight, isomer **8b**$^+$ rearranges to form the formylmethyl hydroxy complex **9b**$^+$. This rearrangement is three times faster than the rearrangement of **8a**$^+$ to **9a**$^+$. The iridadioxolanes are much more reactive than the corresponding rhodadioxolanes, whereas the iridium formylmethyl hydroxy complexes are less reactive than the corresponding rhodium formylmethyl hydroxy complexes. The tpa formylmethyl hydroxy complexes react reversibly with carbon dioxide to form formylmethyl hydrogen carbonate complexes.

Introduction

Transition metal catalyzed oxidation of olefins is one of the most important methods of converting these readily available and cheap starting materials into useful chemicals. For economical and environmental reasons, molecular oxygen or air are the most interesting oxidants. However, not much is known about the mechanisms involved in transition metal catalyzed olefin oxidations. In an attempt to investigate the validity of some of the earlier proposed mechanisms, we have investigated the oxygenation of rhodium and iridium ethene complexes by air.

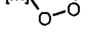

3-Metalla-1,2-dioxolanes (κ^2-C^1,O^2-2-peroxyethyl metal complexes, see Structure) have been proposed as intermediates in the catalytic oxygenation of olefins by group VI and VIII metals.[1] These reactions include epoxidation[1d−1f] and oxidation to ketones.[1a−1c] Mimoun et al. have proposed that the rhodium-catalyzed olefin oxidation proceeds via a peroxo ethene complex. Insertion of ethene into the rhodium dioxygen bond then results in the formation of a 3-rhoda-1,2-dioxolane complex, which subsequently decomposes to acetaldehyde and a rhodium oxo complex (Scheme 1).[1a]

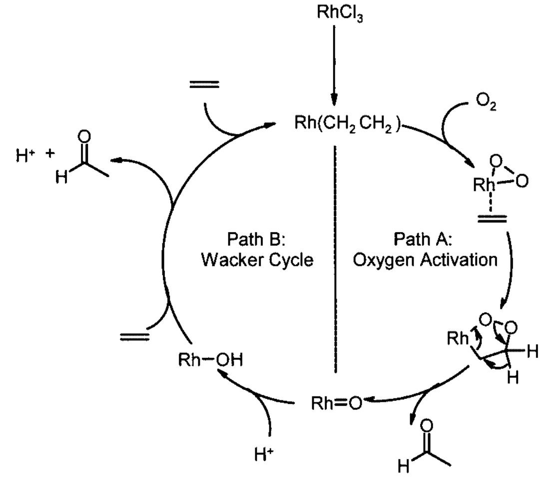

Scheme 1. Mechanism proposed by Mimoun for the rhodium catalyzed oxidation of ethene to acetaldehyde[1a]

---

[a] Department of Inorganic Chemistry, University of Nijmegen
Toernooiveld 1, 6525 ED Nijmegen, The Netherlands
Fax: (internat.) +31-24355-3450
E-mail: gal@sci.kun.nl

Supporting information for this article is available on the WWW under http://www.eurjic.org or from the author.

In the molybdenum catalyzed oxidation of olefins, Mimoun proposed that decomposition of 3-molybdena-1,2-dioxolanes results in the formation of a molybdenum oxo complex and ethylene oxide.[1e][1f] However, calculations by Frenking et al. have indicated that this would lead to the formation of acetaldehyde instead of ethylene oxide.[2]

3-Metalla-1,2-dioxolanes containing an *unsubstituted* 3-metalla-1,2-dioxolane fragment [M($\kappa^2 C^1, O^2$-CH_2CH_2OO-)] have not been reported before. However, tri- and tetra-substituted 3-platina-1,2-dioxolanes, with substituents that prevent β-hydrogen transfer, have been obtained from the reaction of [$(PPh_3)_2Pt(\eta^2$-$O_2)$] with electron-deficient olefins, and have been structurally characterized (**1** and **2**).[3] These *substituted* platinadioxolanes cannot be used as models for the further study of proposed metalladioxolane intermediates.

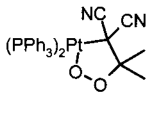

1

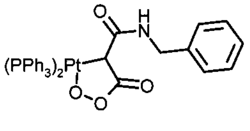

2

We now report on the synthesis of *unsubstituted* 3-metalla-1,2-dioxolanes, through the oxidation of rhodium and iridium ethene complexes by air or molecular oxygen. Oxidation by molecular oxygen was sometimes necessary due to the reactivity of the oxidation products towards water or carbon dioxide from the air. Rearrangement of the 3-metalla-1,2-dioxolanes to formylmethyl hydroxy complexes is also reported. Part of this work has been communicated previously.[4]

Results and Discussion

Synthesis of Ethene Complexes

Rhodium tpa Complexes

The complexes [(tpa)Rh(CH_2CH_2)]BPh_4 {**7**BPh_4, tpa = tris(2-pyridylmethyl)amine} and [(Metpa)Rh(CH_2CH_2)]PF_6 {**14**PF_6, Metpa = [(6-methyl-2-pyridyl)methyl]bis(2-pyridylmethyl)amine} were synthesized according to a literature procedure. $NaBPh_4$ and KPF_6 were used to precipitate **7**BPh_4 and **14**PF_6, respectively.[5]

Iridium tpa Complexes

Bis(ethene) complexes **3**BPh_4 and **3**PF_6 were synthesized from in situ generated $IrCl(C_2H_4)_4$, tpa, and $NaBPh_4$ or KPF_6, respectively. Whereas a mono-ethene complex (**7**$^+$) is formed for rhodium, a bis(ethene) complex is initially obtained for iridium, probably due to the better π-back-donating ability of iridium. However, an ethene molecule is easily lost from the bis(ethene) complex; when N_2 is bubbled through a solution containing **3**$^+$, the mono-ethene complex **4**$^+$ is obtained (Scheme 2). This reaction is reversible; when ethene is bubbled through a solution containing **4**$^+$, the bis(ethene) complex **3**$^+$ is obtained.

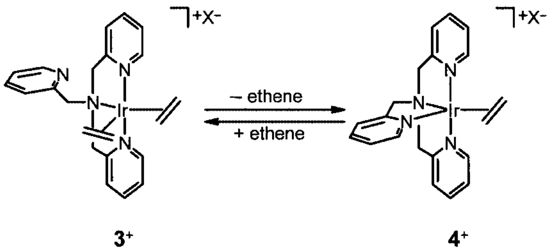

Scheme 2. Reactivity of bis(ethene) complex **3**PF_6 and mono-ethene complex **4**PF_6

The structure of complex **3**$^+$, as determined by X-ray diffraction, is shown in Figure 1. The complex has a trigonal bipyramidal conformation and contains the tpa ligand in a meridional tridentate coordination mode. This coordination mode has not been observed before for bis(olefin) metal complexes stabilized by bpa-type ligands {bpa = bis(2-pyridylmethyl)amine}; in such complexes the bpa-type tridentate nitrogen donor ligand usually adopts a facial coordination mode.[6,7] The ^1H NMR spectrum of **3**$^+$ at room temperature shows four triplets and its ^{13}C NMR spectrum shows four singlets for the ethene fragments, indicating that the fragments are not rotating, probably due to steric hindrance.

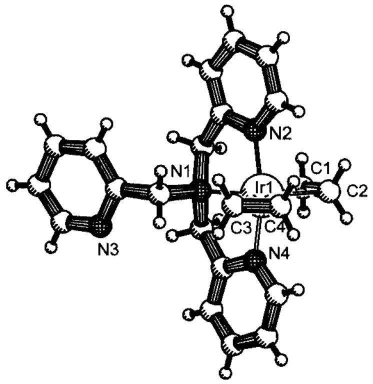

Figure 1. X-ray structure of bis(ethene) complex **3**$^+$

Rhodium N_4Me_2 Complexes

To test the influence of the nitrogen donor ligand on the reactivity of the ethene complexes, bis(ethene) complex **5**$^+$ (Scheme 3) was synthesized as the PF_6-salt from [{(ethene)$_2$RhCl}$_2$], N_4Me_2 and KPF_6. Complex **5**$^+$ contains the rigid macrocyclic N_4 ligand, *N,N′*-dimethyl-2,11-diaza[3,3](2,6)pyridinophane[8] (N_4Me_2). As mentioned earlier, reaction of tpa with $IrCl(C_2H_4)_4$ initially gives a bis(ethene) complex, which easily and reversibly loses one ethene molecule. The same reaction with [{$(C_2H_4)_2RhCl$}$_2$] only produces the mono-ethene complex **7**$^+$, even when carried out at low temperature. Rhodium apparently does not bind the second ethene molecule as strongly as iridium. Therefore, the initial formation of the bis(ethene) complex **5**PF_6 with N_4Me_2 was surprising. However, **5**PF_6 also loses an ethene molecule easily (see below). The synthesis of **5**PF_6 is discussed in more detail in the supporting information.

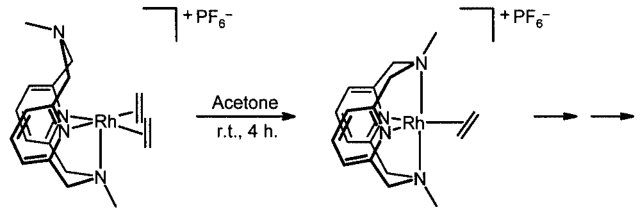

5+ 6+

Scheme 3. Loss of ethene from bis(ethene) complex **5**PF$_6$

The ^{1}H NMR and ^{13}C NMR resonances of the vinylic groups of **5**$^+$ are broad at room temperature, which indicates the rotation of the ethene fragments. At −60 °C this rotation is frozen, resulting in an ABCD-pattern in the ^{1}H NMR spectrum. X-ray quality crystals of **5**PF$_6$ were obtained by crystallization from acetone/diethyl ether (v/v = 1:3) over a period of nine days at −70 °C. The X-ray structure of the cation **5**$^+$ is shown in Figure 2. This is the first reported X-ray structure of a bis(ethene) rhodium complex stabilized by three nitrogen donors.

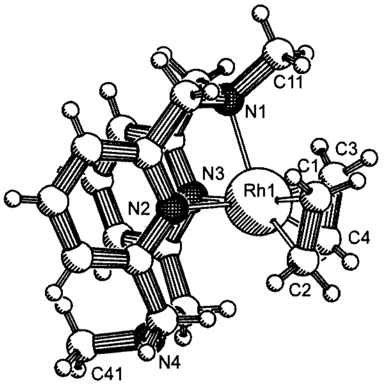

Figure 2. X-ray structure of bis(ethene) complex **5**$^+$

Cation **5**$^+$ has a pseudo square pyramidal geometry with the amine occupying the apical position, and the N$_4$Me$_2$ ligand in a tridentate coordination mode. Three complexes in which this coordination mode is found for N$_4$Me$_2$ (or an analogous ligand) have been reported earlier,[9] but usually this ligand adopts a tetradentate coordination mode.[10] In complex **5**$^+$, as well as in the earlier reported κ^3-N$_4$Me$_2$ complexes,[9] the N$_4$Me$_2$ ligand adopts a *syn* (chair-boat) conformation. The X-ray structure of **5**$^+$ is discussed in more detail in the supporting information.

Mono-ethene complex **6**PF$_6$ is easily obtained by allowing **5**PF$_6$ to stand in acetone solution under a nitrogen atmosphere at room temperature for approximately four hours (Scheme 3). This is not a reversible reaction; bubbling ethene through a solution of **6**PF$_6$, or exposure of such a solution to an ethene atmosphere does not lead to the formation of **5**PF$_6$. The rate and selectivity of the conversion of **5**$^+$ to **6**$^+$ are highly dependent on the counterion used. Formation of **6**$^+$ is slower and more selective if PF$_6^-$ is used as the counterion, instead of BPh$_4^-$. Furthermore, irrespective of the counterion, the selectivity is higher in acetone than in acetonitrile.

Since a square planar [(κ^3-N$_4$Me$_2$)Rh(C$_2$H$_4$)]$^+$ structure is not possible for complex **6**$^+$ due to the rigidity of the N$_4$Me$_2$ ligand, we propose that the ligand has a κ^4-coordination mode, similar to tpa in **7**$^+$.[5] Another indication for tetradentate coordination is the fact that the signals for the NMe groups in the ^{1}H NMR and ^{13}C NMR spectra are at approximately the same chemical shifts [δ(^{1}H) = 2.15 ppm, δ(^{13}C) = 49.8 ppm] as the signals for the coordinated NMe group in **5**$^+$ [δ(^{1}H) = 2.25 ppm, δ(^{13}C) = 52.6 ppm].

Complex **6**PF$_6$ is not stable in solution at room temperature, and decomposes within hours to a mixture of unidentified products. Thus, the formation of **6**PF$_6$ is always accompanied by some decomposition, and analytically pure samples of it and its oxidation products (see below) could not be obtained.

Formation of 3-Metalla-1,2-dioxolanes from Ethene Complexes

Rhodium tpa Complexes

Oxidation of **7**BPh$_4$ by air at room temperature *in solution* (acetone, acetonitrile, dichloromethane) results in the dissociation of ethene and the formation of a mixture of unidentified products. In marked contrast, exposure of *solid* **7**BPh$_4$ to air for two days results in the formation of 3-rhoda-1,2-dioxolane **8a**BPh$_4$ (Scheme 4).[11] A small amount of the hydroperoxy hydroxy complex **25**BPh$_4$ is also formed (see below).

The ESI-MS spectrum of **8a**BPh$_4$ shows a base peak at *m*/*z* = 453, corresponding to [(tpa)Rh(CH$_2$CH$_2$) + O$_2$]$^+$. The ^{1}H NMR spectrum shows the presence of a Rh−CH$_2$−CH$_2$ group. The ^3J(H$_\alpha$,H$_\beta$) coupling constant for this group (6.1 Hz, Table 1) suggests that it is part of a five-membered ring: the coupling constant is intermediate in magnitude between that observed in the four-membered 2-rhodaoxetane ring in **12b**$^+$ and the six-membered ring in the rhodium 2-(acetimidoyloxy)ethyl complex **13b**$^{2+}$ (Scheme 5).[5]

Crystals of **8a**BPh$_4$ suitable for X-ray diffraction were obtained by slow diffusion of diethyl ether into a 1,2-dichloroethane/acetonitrile solution. The unit cell contains two crystallographically independent units, which are almost mirror images. The structure of one of the units is shown in Figure 3. The five-membered ring has an envelope conformation. The puckering of the 3-rhoda-1,2-dioxolane ring is virtually the same as in the 3-platina-1,2-dioxolane ring of **1**.[3a],[12] The average O1−O2 distance [1.500(17) Å] is normal compared with the O−O distances in **1** [1.482(15) Å][3a] and other M−O−O-C compounds (1.40−1.52 Å);[13] the average O2−C2 distance [1.443(10) Å] is also similar to that in **1** [1.407(19) Å] and other M−O−O-C compounds (1.40−1.47 Å).[14]

The nature of the counterion largely influences the selectivity of this solid-gas oxygenation reaction. On changing the counterion of **7**$^+$ from BPh$_4^-$ to PF$_6^-$, a 1:1 mixture of

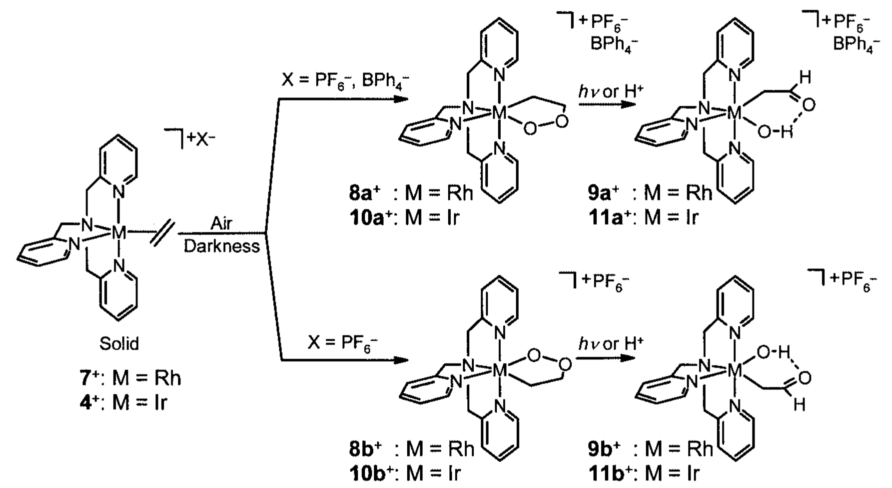

Scheme 4. Formation and rearrangement of 3-metalla-1,2-dioxolanes

Table 1. ^{1}H NMR chemical shifts (ppm) and coupling constants (Hz) of the $RhCH_2CH_nO$ fragments in CD_3CN

Compound	δ(MCH_2)	δ(CH_nO)[a]	$^{3}J_{H,H}$	$^{2}J_{H,Rh}$
8a$^+$	2.57(dt)	3.25(t)	6.1	2.4
8b$^+$	3.55 (dt)	3.41(t)	6.1	2.4
10a$^+$	2.03(t)	2.54(t)	6.2	–
10b$^+$	2.69(t)	2.63(t)	6.7	–
16$^+$	2.90(dt)	3.66(t)	6.5	2.5
12b$^+$	2.24(dt)	4.88(t)	7.5	2.5
9a$^+$	2.69(dd)	9.26(t)	5.1	2.9
9b$^+$	3.47(dd)	9.98(t)	4.9	2.9
11a$^+$	3.07(d)	9.21(t)	5.2	–
11b$^+$	3.66(d)	10.11(t)	4.9	–
17$^+$	3.14(dd)	9.57(t)	5.4	3.2
20a^{2+}	3.05(dd)	9.51(t)	4.9	2.7
21a$^+$	3.23(dd)	9.53(t)	4.7	2.5
22a$^+$	3.39(d)	9.46(t)	4.8	–
18$^+$	3.21(dd)	9.70(t)	5.5	2.8

[a] n = 1,2.

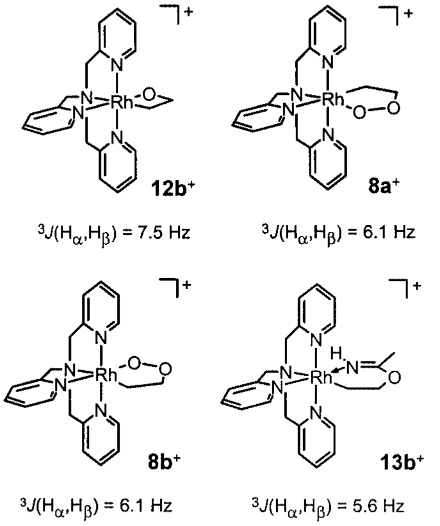

Scheme 5. Typical $^{3}J(H_\alpha,H_\beta)$ for $Rh-CH_2-CH_2$ fragments in four-membered (**12b**$^+$), five-membered (**8a**$^+$, **8b**$^+$), and six-membered (**13b**$^{2+}$) rings

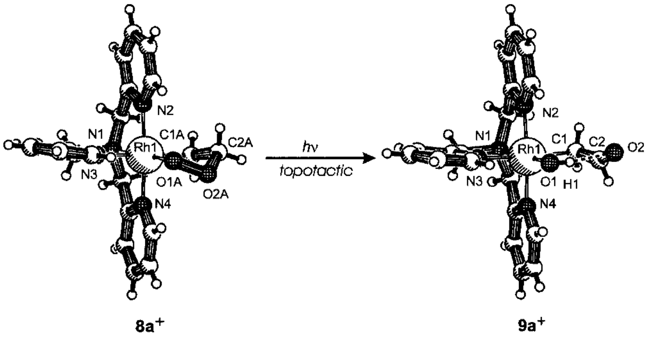

Figure 3. X-ray structures of 3-rhoda-1,2-dioxolane **8a**$^+$ and rhodium formylmethyl hydroxy complex **9a**$^+$

8aPF_6 and a new complex **8b**PF_6 is obtained after exposure to air for two days.[11] The ESI-MS and ^{1}H NMR spectra of the mixture of **8a**PF_6 and **8b**PF_6 in CD_3CN indicate that **8b**$^+$ is the isomeric 3-rhoda-1,2-dioxolane in Scheme 4. The C_α resonances in the ^{13}C NMR spectrum are at δ = 35.0 and δ = 44.8 ppm for **8a**$^+$ and **8b**$^+$, respectively, reflecting the stronger donor capacity of a pyridine versus an amine group (Table 2). The same trend is observed for **9a**$^+$/**9b**$^+$, **10a**$^+$/**10b**$^+$, and **11a**$^+$/**11b**$^+$, which are discussed below.

The NOE contacts in **8a**$^+$ and **8b**$^+$ are consistent with their proposed structures: isomer **8a**$^+$ shows NOE contacts between $Rh-CH_2-CH_2-$ and one proton each of the two equivalent $Rh-N_{amine}-CH_2-$ groups, and between $Rh-CH_2-CH_2-$ and the two equivalent py-H6 atoms; isomer **8b**$^+$ shows NOE contacts between $Rh-CH_2-CH_2-$ and all three py-H6 atoms, and between $Rh-CH_2-CH_2-$ and the two equivalent py-H6 atoms.

Possibly, the different packing in (microcrystalline) **7**BPh_4 and **7**PF_6 leads to the different accessibility of cation **7**$^+$ to O_2. Remarkably, oxidation of **7**$^+$ by hydrogen peroxide only leads to the formation of 2-rhodaoxetane **12b**$^+$ (N_{amine}, *C trans*) (Scheme 5).[5] Thus far, a 2-rhodaoxetane, **12a**$^+$ (N_{amine}, *O trans*), has not been observed.

Besides the influence of the counterion, small ligand changes also have a large effect on the reactivity of *solid* rhodium-ethene complexes towards air. Substitution of one

Table 2. ^{13}C NMR chemical shifts (ppm) and coupling constants (Hz) of the $RhCH_2CH_nO$ fragments in CD_3CN

Compound	δ(MCH_2)	δ(CH_nO)[a]	$^1J_{C,Rh}$
8a$^+$	35.0(d)	70.2(s)	25.0
8b$^+$	44.8(d)	72.8(s)	28.8
10a$^+$	15.8(s)	71.1 or 71.8(s)	–
10b$^+$	23.9(s)	71.6(s)	–
16$^+$	30.3(d)	71.7(s)	25
12b$^+$	1.3(d)[b]	78.7(d)	18.4[b]
9a$^+$	26.9(d)	209.0(s)	21.0
9b$^+$	34.5(d)	210.8(s)	25.0
11a$^+$	16.3(s)	209.4(s)	–
11b$^+$	20.7(s)	211.2(s)	–
17$^+$	33.4(d)	207.7(s)	21.2
20a^{2+}	27.8(d)	206.7(d)	20.4
21a$^+$	28.1(d)	210.1(s)	20.7
22a$^+$	14.8(s)	211.1(s)	–

[a] $n = 1,2$. [b] $[D_6]$Acetone.

Py-H6 of tpa for a methyl group, for example, leads to a large decrease in the reaction rate. According to the ^1H NMR spectrum (Scheme 6), exposure of *solid* **14**PF_6 to pure molecular oxygen for *7 months* results in approximately 45% conversion into a 2:1 mixture of **15a**$^+$ and **15b**$^+$ (the remainder being starting material). Exposure of *solid* **14**BPh_4 to pure molecular oxygen for a similar period of time also results in the formation of a mixture of **15a**$^+$ and **15b**$^+$. This was unexpected since exposure of the analogous complex **7**BPh_4 only results in the formation of isomer **8a**$^+$. Again, different packing in **7**BPh_4 and **14**BPh_4 might be responsible for this difference in selectivity.

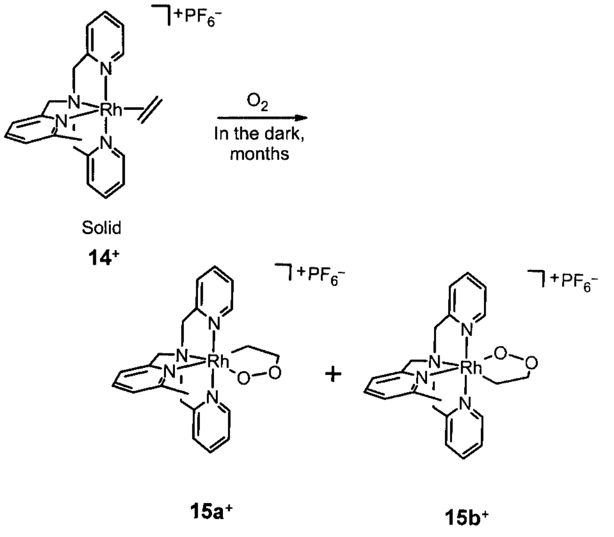

Scheme 6. Oxygenation of rhodium ethene complex **14**PF_6

Iridium tpa Complexes

Exposure of a *solution* of **4**BPh_4 to air leads to a mixture of unidentified products, whereas exposure of *solid* **4**BPh_4 to air leads to the formation of 3-irida-1,2-dioxolane **10a**BPh_4 (Scheme 4). Exposure of *solid* **4**PF_6 to air results in the formation of a mixture of the isomeric iridadioxolanes **10a**PF_6 and **10b**PF_6, in an approximate ratio of 2:5 (Scheme 4). Powder X-ray diffraction spectra of **4**PF_6 and **7**PF_6 show that these complexes are isomorphous, which indicates that the different ratios in which the isomeric 3-rhoda- and 3-iridadioxolanes are formed do not stem from the different packing of the starting materials.

ESI-MS spectra of **10a**BPh_4 and **10a**PF_6/**10b**PF_6 could not be obtained because of the instability of these complexes in solution at room temperature (see below). The ^1H NMR spectra show two triplets for the $Ir-CH_2-CH_2-$ fragment, with $^3J(H_\alpha,H_\beta) = 6.2$ and 6.7 Hz for **10a**$^+$ and **10b**$^+$, respectively. This indicates that the fragments are part of five-membered rings (Table 1, Scheme 5). The ^1H NMR signals for $IrCH_2$- and for $-CH_2O-$ were assigned by analogy with the 3-rhoda-1,2-dioxolanes (Table 1).

Rhodium N₄Me₂ Complexes

On reaction of *solid* **6**PF_6 with dioxygen (instead of air; see below), at room temperature in the dark, **16**PF_6 was formed within a few days.[11] The ^1H NMR spectrum of **16**PF_6 shows two double triplets at $\delta = 2.94$ ppm and at $\delta = 3.70$ ppm, indicating the presence of a $RhCH_2CH_2X$ fragment (Table 1). A coupling constant of $^3J_{H,H} = 6.5$ Hz for these signals indicates that a five-membered ring is formed (Table 1). The ESI-MS spectrum shows a base peak at $m/z = 431$, which is in accordance with the formation of 3-rhodadioxolane **16**$^+$ (Scheme 7). All attempts to obtain X-ray quality crystals of **16**$^+$ failed, partly because of its instability in solution.

Rearrangement of 3-Metalla-1,2-dioxolanes to Formylmethyl Hydroxy Complexes

Rhodium tpa Complexes

Exposure of microcrystalline **8a**BPh_4 to glass-filtered daylight under N_2 results in the selective conversion into the corresponding rhodium formylmethyl hydroxy complex **9a**BPh_4, in several weeks (Scheme 4). Similarly, exposure of a solution of **8a**BPh_4 in CD_3CN to the glass-filtered light of a high-pressure mercury lamp at −30 °C results in the conversion into **9a**BPh_4. Monitoring of this reaction by ^1H NMR indicates that an optimum yield of 90% **9a**BPh_4 is obtained after 90 minutes of illumination (see Supporting Information).

The ESI-MS spectrum of **9a**$^+$ is similar to that of **8a**$^+$, with the exception of a peak at $m/z = 435$, which corresponds to the loss of water from the parent cation. Such loss of water in the gas-phase has been observed earlier for the transient formylmethyl hydroxy complex $[(MeCN)(Bzbpa\text{-}\kappa^3)Rh(CH_2CHO\text{-}\kappa^1)(OH)]BPh_4$ (**19**BPh_4), which is the only other formylmethyl hydroxy complex reported thus far,[15,16] although several other formylmethyl complexes have been reported.[17]

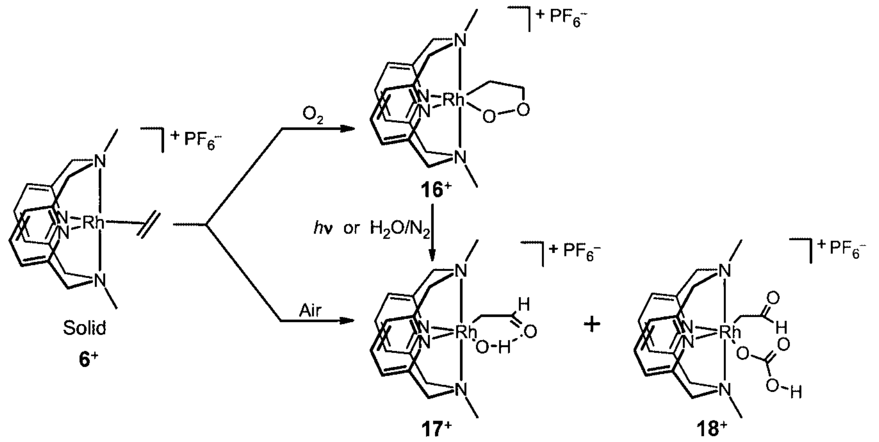

Scheme 7. Formation and rearrangement of rhodadioxolane **16**PF$_6$ and subsequent reaction with CO$_2$

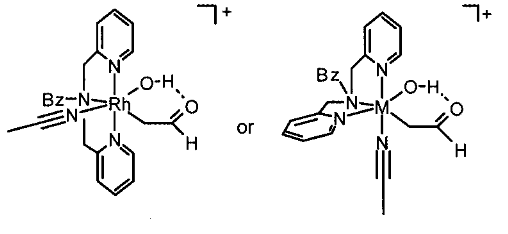

19$^+$

The ^{1}H NMR and ^{13}C NMR spectra of **9a**BPh$_4$ show signals typical of a metal-bound formylmethyl group, similar to those found in **19**BPh$_4$ (Tables 1 and 2).[16] Complex **9a**$^+$ shows a strong IR absorption at 1655 cm^{-1}, in accordance with the presence of a carbonyl group.

After repeated attempts to obtain X-ray quality crystals of **9a**BPh$_4$ had failed, an attempt was made to photochemically convert a single crystal of **8a**BPh$_4$ to a single crystal of **9a**BPh$_4$. The crystal that had been used for the X-ray structure determination of **8a**BPh$_4$ was exposed to glass-filtered daylight for one week and its crystal structure was re-determined. It was found that **8a**$^+$ had been fully converted into **9a**$^+$ leaving the crystal packing virtually unchanged (a "topotactic" transformation).[18]

The crystal structure of **9a**$^+$ shows that the hydroxy group forms a hydrogen-bond with the formyl fragment, thus forming a puckered six-membered ring (Figure 3). The bridging hydrogen (H1) was refined at an O1−H1 distance of 0.80(5) Å [Rh−O1−H1 = 99(4)°] and a H1−O2 distance of 1.92(5) Å [O1−H1−O2 = 168(5)°]. The puckering of the six-membered ring results from the rotation of the formyl fragment around the C1−C2 bond [torsion angle Rh−C1−C2−O2 = −72(3)°]. The crystal structure of **9a**$^+$ is discussed in more detail in the supporting information.

We propose that the photochemical rearrangement of **8a**$^+$ to **9a**$^+$ involves photolysis of the O−O bond, followed by abstraction of a β-hydrogen atom from $-CH_2-CH_2-O^{\cdot}$ by $-O^{\cdot}$ (Scheme 8, a). In the solid state, the puckering of the 3-rhoda-1,2-dioxolane ring positions a β-hydrogen in close proximity of the O1 atom (Figure 3). Therefore, this reaction would not be hindered by the constraints of the lattice. The mechanism, shown in Scheme 8 (see a), is supported by preliminary DFT calculations.[19]

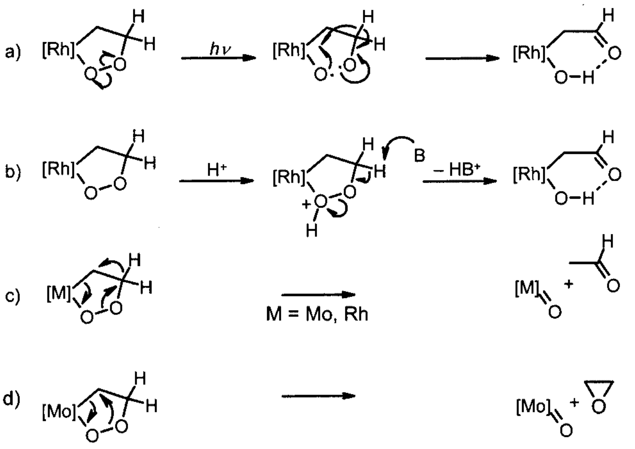

Scheme 8. Proposed mechanisms for rearrangement of 3-metalla-1,2-dioxolanes: a) photochemically, to a formylmethyl hydroxy complex b) proton assisted, to a formylmethyl hydroxy complex c) directly, to an oxo complex species and acetaldehyde[1a,2] and d) directly, to an oxo complex and ethylene oxide[1f]

Analogous to microcrystalline 3-rhoda-1,2-dioxolane **8a**BPh$_4$, the microcrystalline mixture of the isomeric 3-rhoda-1,2-dioxolanes **8a**PF$_6$ and **8b**PF$_6$ (**8a**PF$_6$/**8b**PF$_6$) rearranges photochemically to a mixture of the isomeric formylmethyl hydroxy complexes **9a**PF$_6$ and **9b**PF$_6$ (**9a**PF$_6$/**9b**PF$_6$; Scheme 4). However, **8a**BPh$_4$ and **8a**PF$_6$/**8b**PF$_6$ react differently when exposed to a N$_2$ atmosphere saturated with H$_2$O; complex **8a**BPh$_4$ proved to be stable, whereas **8a**PF$_6$/**8b**PF$_6$ rearranges to **9a**PF$_6$/**9b**PF$_6$. Since **8a**PF$_6$/**8b**PF$_6$ is stable under dry N$_2$, this reactivity must have been triggered by the presence of H$_2$O. Since there is no obvious mechanism by which H$_2$O would directly cause O−O bond breaking in the rhodadioxolane, we considered the possibility that a trace of acid (possibly generated from hydrolysis of a small amount of PF$_6^-$ to PF$_2$O$_2^-$ and HF) catalyzes the conversion. To investigate proton-assisted ring opening in solution, 0.1 equivalent of the noncoordinating acid [H(OEt$_2$)$_2$]B[C$_6$H$_3$(CF$_3$)$_2$]$_4$ ($HBAr^F_4$) was added to a solution of **8a**BPh_4 in CD_3CN. In a typical experiment, the ^1H NMR spectrum shows that **8a**$^+$ is converted into the formylmethyl hydroxy complex **8a**$^+$ (87%) within 10 minutes, and a small amount (8%) of the formylmethyl aqua complex **20a**$^{2+}$ (i.e. protonated **9a**$^+$) is also formed.[20] Likewise, addition of 1.1 equivalent of $HBAr^F_4$ to a solution of **8a**BPh_4 results in the formation of **20a**$^{2+}$ in approximately 85% yield within 10 minutes.[20] In the latter case, any **9a**$^+$ formed is apparently directly protonated. This protonation results in a downfield shift of the $Rh-CH_2-CHO$ and $Rh-CH_2-CHO$ ^1H NMR signals from $\delta = 2.69$ to $\delta = 3.05$ ppm and from $\delta = 9.26$ to $\delta = 9.51$ ppm, respectively. The base-peak in the ESI-MS spectrum of the obtained solution has the correct isotope distribution pattern and *m/z* value (227) for **20a**$^{2+}$. As demonstrated by its formylmethyl ^1H NMR signals, a trace of **20a**$^{2+}$ is also formed in the conversion of *solid* **8a**PF_6/**8b**PF_6 to **9a**PF_6/**9b**PF_6 under N_2 saturated with H_2O. This supports our hypothesis of an acid-catalyzed ring opening.

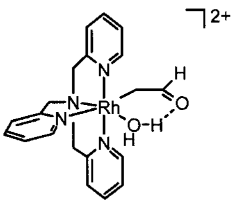

20a^{2+}

A possible mechanism for the acid-catalyzed ring opening is shown in Scheme 8, b. Protonation of **8a**$^+$ at O_α induces heterolytic splitting of the O−O bond, followed by the deprotonation at C_β by an external base and the formation of a carbonyl double bond. This mechanism was supported by preliminary DFT calculations.[19]

The isomeric 3-rhodadioxolanes **8a**$^+$ and **8b**$^+$ clearly differ in their photoreactivity: on exposure of a CD_3CN solution of **8a**$^+$ and **8b**$^+$ to glass-filtered daylight at room temperature, the relative intensities of the ^1H NMR 2-peroxyethyl signals show that the initial reaction rate of **8b**$^+$ is three times faster than that of **8a**$^+$ (Figure 4).

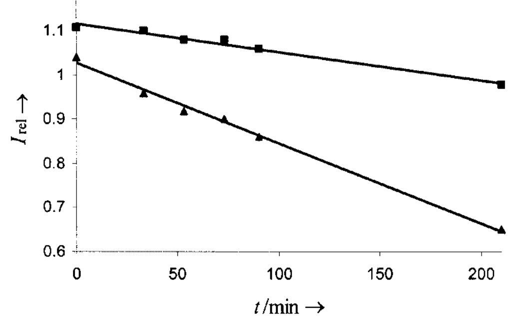

Figure 4. Relative intensities of the 2-peroxyethyl ^1H NMR signals of **8a**$^+$ (■) and **8b**$^+$ (▲) on exposure to glass-filtered daylight

Formylmethyl hydroxy complexes **9a**$^+$ and **9b**$^+$ decompose to a mixture of unidentified products in solution at room temperature on prolonged exposure to light.

Iridium tpa Complexes

Both **10a**$^+$ and **10b**$^+$ rearrange to iridium formylmethyl hydroxy complexes (**11a**$^+$ and **11b**$^+$) on exposure to light. The ESI-MS spectra of **11a**BPh_4 and **11a**PF_6/**11b**PF_6 show the expected base peak at *m/z* = 543. For **11a**BPh_4, the daughter ion spectrum from this base peak shows a peak at *m/z* = 525, corresponding to the loss of water.

There is a large difference in reactivity between the 3-rhodadioxolanes and the 3-iridadioxolanes: 3-iridadioxolanes rearrange to form formylmethyl hydroxy complexes in solution at room temperature, whereas 3-rhodadioxolanes need to be exposed to light or protons before rearrangement can take place. It is possible that the iridadioxolanes are more sensitive to traces of adventitious acid, e.g. on glass surfaces, than the rhodadioxolanes. Another possibility is that for iridium, water is already a strong enough acid to induce the conversion. Finally, an alternative conversion mechanism, not requiring any acid, may be possible for iridium.

The iridium formylmethyl hydroxy complexes **11a**$^+$ and **11b**$^+$ are stable in CH_3CN solution at room temperature when exposed to light, whereas the rhodium analogues decompose under these conditions.

Rhodium N_4Me_2 Complexes

Both in the presence and absence of visible light, the *solid* mono-ethene complex **6**PF_6 reacts with air, within a few days at room temperature, to form a mixture of two formylmethyl complexes in an approximate ratio of 5:1, according to the ^1H NMR spectrum in CD_3CN. The ESI-MS spectrum of the mixture in CH_3CN shows a base peak at *m/z* = 431, in accordance with the presence of the formylmethyl hydroxy complex **17**$^+$, and a peak at *m/z* = 475, corresponding to the formylmethyl hydrogen carbonate complex **18**$^+$. Water present in the air probably induces an acid-catalyzed rearrangement of the initially formed dioxolane to a formylmethyl hydroxy complex. Although rearrangement on exposure to a nitrogen atmosphere saturated with water had been observed earlier for the tpa complexes (see above), rearrangement on exposure to air was not observed. Furthermore, the resulting formylmethyl hydroxy complex reacts with carbon dioxide from the air, forming **18**$^+$. This has not been observed for the tpa complexes either. However, exposure of **9a**BPh_4 or **11a**BPh_4 to a CO_2 atmosphere leads to the full conversion into the formylmethyl hydrogen carbonate complexes **21a**BPh_4 and **22a**BPh_4, respectively (Scheme 9). On removal of the CO_2 atmosphere, CO_2 is released and the formylmethyl hydroxy complexes **9a**BPh_4 or **11a**BPh_4 are regenerated. Formation of rhodium and iridium hydrogen carbonate complexes from metal hydroxy complexes and CO_2, and vice versa have been reported before.[21]

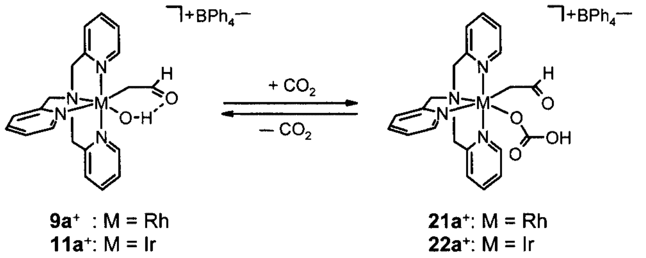

Scheme 9. Reversible reaction of formylmethyl hydroxy complexes **9a**$^+$ and **11a**$^+$ with CO_2

Exposure of *solid* **16**PF_6 (obtained from **6**PF_6 and dioxygen; see above) to visible light and N_2 leads to the conversion into **17**PF_6, as shown by the ESI-MS, ^1H NMR and ^{13}C NMR spectra in CD_3CN (Tables 1 and 2). Exposure of **16**PF_6 to water vapour/N_2 also leads to the formation of **17**PF_6, probably due to the PF_6^- counterion (see above).

Oxidation of a Rhodium Propene Complex to a Peroxo Complex and Its Reactivity towards Water

As mentioned earlier, exposure of *solid* **7**BPh_4 to air not only produces 3-rhoda-1,2-dioxolane **8a**BPh_4, but also a small amount of the hydroperoxy hydroxy complex **25**BPh_4. Exposure of *solid* **7**BPh_4 to pure dioxygen, however, leads to the formation of **8a**BPh_4 and a small amount of the peroxo complex **24**BPh_4. This peroxo complex can be obtained more efficiently by the oxidation of *solid* [(tpa)Rh-(CH_2CHCH_3)]BPh_4 (**23**BPh_4) with molecular oxygen (Scheme 10).

Complex **23**BPh_4 was synthesized from [{(ethene)$_2$-RhCl}$_2$], propene, tpa, and $NaBPh_4$. It is the first reported rhodium propene complex stabilized by a tetradentate nitrogen donor ligand. Propene coordinates less strongly to the rhodium center than ethene, resulting in an easier loss of olefin from the complex and the quantitative formation of **24**BPh_4 on oxidation with molecular oxygen. Oxidation with air results in a mixture of unidentified products. The reason for this is still unclear. Possibly, further reactions of **24**BPh_4 with water (see below), and subsequently with CO_2 occur. The ^1H NMR and ^{13}C NMR spectra of **24**BPh_4 only show signals for the (coordinated) tpa ligand. The ESI-MS spectrum of **24**BPh_4 shows a base peak at *m/z* = 425, corresponding to [(tpa)Rh + O_2]$^+$, and the loss of O_2 from the parent cation.[22]

Exposure of complex **24**BPh_4 to a nitrogen atmosphere saturated with water leads to the complete conversion into **25**BPh_4. The ^1H NMR and ^{13}C NMR spectra of **25**BPh_4 again only show signals for the (coordinated) tpa ligand. The ESI-MS spectrum shows a base peak at *m/z* = 443, corresponding to **25**$^+$, and the loss of H_2O, HO_2, and H_2O_3 from the parent cation. Complex **25**BPh_4 is the first rhodium hydroperoxy hydroxy complex reported, but other metal hydroperoxy hydroxy complexes have been reported earlier.[23] Analytically pure samples of **24**BPh_4 and **25**BPh_4 were not obtained, due to their instability in solution at room temperature. Since the decomposition of **25**BPh_4 is a problem in solution at −30 °C as well, no ^{13}C NMR spectroscopic data were obtained for this complex.

Conclusions

We have achieved selective oxidation of [M]^I(ethene) (M = Rh, Ir) complexes by air or dioxygen to form isolable 3-metalla-1,2-dioxolanes for the first time. Remarkably selective dioxygenation was only achieved for ethene complexes embedded in a crystalline matrix. The reasons for this difference between solid phase reactivity and solution phase reactivity have not yet been elucidated. However, our results clearly indicate that solid-gas reactions should be considered as a useful alternative to conventional solution phase chemistry, not only under heterogeneous conditions (high pressures and temperatures), but also at room temperature and atmospheric pressure.

Small changes have a large effect on the reactivity of the ethene complexes. The dioxygenation of **14**PF_6 is much slower than of **7**PF_6. Using a completely different N_4-ligand (N_4Me_2) results in a higher reactivity of not only the ethene

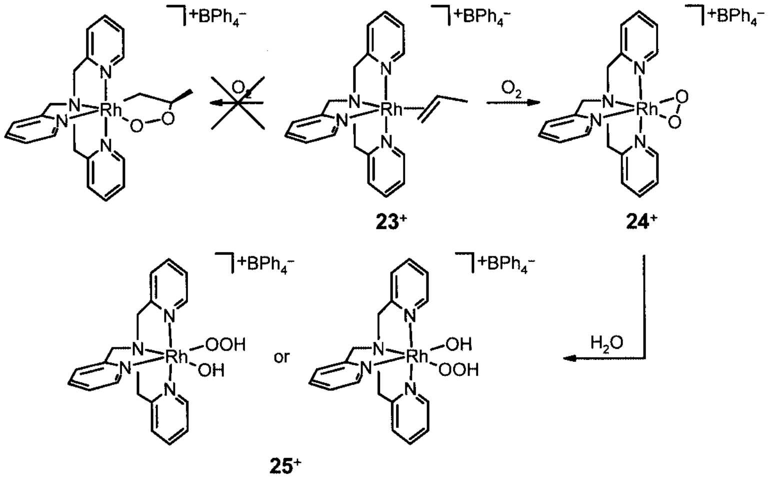

Scheme 10. Reaction of propene complex **23**BPh_4 with dioxygen

complex, but also of the 3-rhodadioxolane and the formylmethyl hydroxy complex. More interestingly, even the counterion affects the oxidation chemistry; oxygenation of **7**PF_6 results in the formation of two isomeric 3-rhodadioxolanes, whereas oxygenation of **7**BPh_4 only yields one isomer. Thus, it appears that for these solid-gas reactions, new opportunities for reaction tuning exist.

The observed rearrangement of 3-metalla-1,2-dioxolanes to formylmethyl hydroxy complexes is in marked contrast with the rearrangements proposed earlier for 3-metalla-1,2-dioxolanes i.e. direct rearrangement to a metal oxo complex and acetaldehyde, or to a metal oxo complex and ethylene oxide.[1f] However, the formylmethyl complexes may still be intermediates in the formation of acetaldehyde and a rhodium oxo or hydroxy complex.

In the 1980's Read et al. proposed that 3-rhodadioxolanes are intermediates in the co-oxygenation of terminal or cyclic olefins and triphenylphosphane, to ketones and triphenylphosphane oxide (Scheme 11).[1b] The 3-rhodadioxolane is converted into a 2-rhodaoxetane via the transfer of an O atom to triphenylphosphane. The triphenylphosphane oxide stabilized 2-rhodaoxetane then successively loses triphenylphosphane oxide and a ketone. Our findings do not support such a mechanism. 3-Rhoda-1,2-dioxolane **8a**BPh_4 does not react with triphenylphosphane, and the formation of 2-rhodaoxetanes from 3-rhoda-1,2-dioxolanes have not been observed.

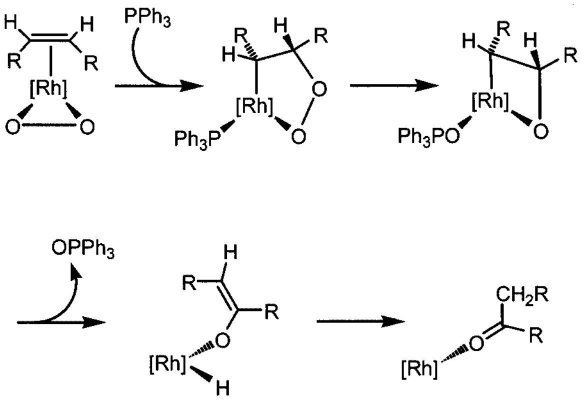

Scheme 11. Mechanism proposed by Read for rhodium catalyzed co-oxygenation of olefins and triphenylphosphane to ketones and triphenylphosphane oxide[1b]

Both Mimoun and Read proposed the formation of 3-rhoda-1,2-dioxolanes from rhodium peroxo ethene complexes.[1a,1b] We have not observed such peroxo ethene intermediates in the formation of 3-rhoda-1,2-dioxolanes. Our group has isolated iridium peroxo ethene complexes, generated through the reaction of iridium ethene complexes with dioxygen in solution, however, these complexes are quite stable and the formation of 3-irida-1,2-dioxolanes is not observed from these complexes.[6c]

Experimental Section

General Methods: All procedures were performed under a nitrogen atmosphere using standard Schlenk techniques, unless indicated otherwise. The solvents (p.a.) were deoxygenated by bubbling through a stream of nitrogen.

NMR experiments were carried out on Bruker DPX200, Bruker AC300, Bruker WM400, and Bruker AM-500. Solvent shift references for ^1H NMR are: CD_2Cl_2 $\delta(^1H)$ = 5.31 ppm, CD_3CN $\delta(^1H)$ = 1.94 ppm and $[D_6]$acetone $\delta(^1H)$ = 2.05 ppm. Solvent shift references for ^{13}C NMR are: CD_3CN $\delta(^{13}C)$ = 118.1 ppm and $[D_6]$acetone $\delta(^{13}C)$ = 206.18 ppm. Abbreviations used are: s = singlet, d = doublet, dd = double doublet, t = triplet, dt = double triplet, q = quadruplet, qq = quadruplet of quadruplets, m = multiplet, dm = double multiplet, br. = broad. Mass spectra (ESI) were recorded on a Finnigan MAT 900S and a Finnigan TSQ 7000 mass spectrometer. Elemental analyses (C, H N) were carried out on an Hanau Elementar-Analyzer CHN-O-Rapid. Infrared spectra were measured on a Perkin−Elmer 1720X spectrometer.

Compounds $[\{(CH_2CH_2)_2RhCl\}_2]$,[24] tpa,[25] Metpa,[26] $[(Me\text{-}tpa)Rh(CH_2CH_2)]BPh_4/PF_6$,[5] $[(tpa)Rh(CH_2CH_2)]BPh_4/PF_6$,[5] N_4Me_2,[27] $[\{(C_8H_{14})IrCl\}_2]$,[28] and $[H(OEt_2)_2]B[C_6H_3(CF_3)_2]_4$ ($HBAr^F_4$)[29] were prepared according to literature procedures. All other chemicals were obtained commercially and were used without further purification.

X-ray Diffraction: Crystals of **3**PF_6 suitable for X-ray diffraction were obtained by slow diffusion of diethyl ether into an acetonitrile solution. Crystals of **5**PF_6 were obtained by crystallization from acetone/diethyl ether (v/v = 1:3) over a period of nine days at −70 °C. Crystals of **8a**BPh_4 were obtained through slow diffusion of diethyl ether into a 1,2-dichloroethane/acetonitrile solution. A crystal of **9a**BPh_4 was obtained by exposure of a crystal of **8a**BPh_4 to glass-filtered daylight for one week.

X-ray diffraction data for **3**PF_6 and **5**PF_6 were collected at 208(2) K on an Enraf−Nonius CAD4 diffractometer, using graphite monochromatized Mo-K_α radiation (λ = 0.71073 Å) and Cu-$K\alpha$ radiation (λ = 1.54184 Å), respectively. X-ray diffraction data for **8a**BPh_4 and **9a**BPh_4 were collected at 150(2) K on a Nonius KappaCCD diffractometer with rotating anode, using graphite monochromatized Mo-K_α radiation (λ = 0.71073 Å). The structures were solved by the PATTY[30] option of the DIRDIF[31] program system. All non-hydrogen atoms were refined with anisotropic temperature factors. The bridging hydrogen atom of the formyl fragment in **9a**BPh_4 was taken from a difference Fourier map and was freely refined. All other hydrogen atoms were placed at calculated positions and were refined isotropically in riding mode. Subsequently, for **5**PF_6, the hydrogen atoms were freely refined. Selected bond lengths and angles are shown in Tables 3 and 4. Other relevant crystal data are summarized in Table 5. Drawings were generated with the program PLATON.[32]

3PF_6**:** Geometrical calculations (PLATON, Spek 1995)[33] revealed neither unusual geometric features, nor unusual short intermolecular contacts. The calculations revealed no higher symmetry and no solvent accessible areas.

5PF_6**:** There is a disordered solvent molecule present in the crystal structure. Calculations (PLATON, Spek,1995)[33] showed a void of 95 Å^3, containing 31 electrons, at 0.0032, 0.466, 0.842. Based on the synthetic route, the electron density most probably represents one acetone molecule (C_3H_6O, 32 electrons). The SQUEEZE pro-

Table 3. Selected bond lengths [Å] for **3**$^+$, **5**$^+$, **8a**A$^+$, **8a**B$^+$, and **9a**$^+$ (M = Rh or Ir)

	3$^+$	**5**$^+$	**8a**A$^+$	**8a**B$^+$	**9a**$^+$
N1−M	2.175(8)	2.311(5)	2.054(2)	2.054(2)	2.040(3)
N2−M	2.027(10)	2.145(5)	2.015(3)	2.015(3)	2.018(4)
N3−M	−	2.163(5)	2.133(3)	2.133(3)	2.102(3)
N4−M	2.056(8)	−	2.030(3)	2.030(3)	2.033(4)
C1−M	2.164(11)	2.113(7)	2.030(16)	2.076(16)	2.085(4)
C2−M	2.126(13)	2.143(7)	−	−	−
C3−M	2.157(11)	2.104(8)	−	−	−
C4−M	2.118(10)	2.125(8)	−	−	−
O1−M	−	−	2.01(2)	1.97(2)	2.014(3)
O1−O2	−	−	1.504(18)	1.496(16)	−
O1−H1	−	−	−	−	0.80(5)
H1−O2	−	−	−	−	1.92(5)
O2−C2	−	−	1.430(11)	1.455(9)	1.103(11)
C2−C1	1.419(16)	1.411(11)	1.563(11)	1.534(11)	1.245(12)
C3−C4	1.416(16)	1.341(11)	−	−	−

Table 4. Selected angles and torsion angles [°] for **3**$^+$, **5**$^+$, **8a**A$^+$, **8a**B$^+$, and **9a**$^+$ (M = Rh or Ir)

	3$^+$	**5**$^+$	**8a**A$^+$	**8a**B$^+$	**9a**$^+$
N1−M−N2	82.2(3)	78.41(19)	84.04(10)	84.04(10)	83.54(13)
N1−M−N3	−	78.2(2)	81.87(10)	81.87(10)	82.83(12)
N1−M−N4	82.1(3)	−	82.91(10)	82.91(10)	82.44(13)
N2−M−N3	−	77.72(19)	88.47(10)	88.47(10)	87.78(13)
N2−M−N4	164.1(4)	−	166.33(10)	166.33(10)	165.46(13)
N3−M−N4	−	−	93.70(10)	93.70(10)	94.27(13)
C1−M−O1	−	−	84.6(4)	84.7(4)	90.18(18)
C2−C1−M	69.2(6)	71.8(4)	106.0(9)	102.2(8)	111.4(5)
O2−C2−C1	−	−	106.2(18)	111.5(10)	146(2)
O1−O2−C2	−	−	106.1(15)	101.7(11)	−
M−O1−O2	−	−	106.3(10)	110.8(12)	−
C1−M−N1	95.7(4)	95.3(3)	99.3(3)	95.9(3)	96.18(15)
C1−M−N2	89.4(4)	96.7(3)	91.2(4)	87.5(4)	89.26(16)
C1−M−N3	−	172.1(3)	178.7(3)	175.6(4)	176.97(16)
C1−M−N4	90.1(4)	−	86.9(4)	89.8(4)	88.44(17)
O1−M−N1	−	−	175.9(4)	179.1(7)	173.63(15)
O1−M−N2	−	−	97.0(12)	95.3(11)	96.19(15)
O1−M−N3	−	−	94.2(3)	97.5(3)	90.80(15)
O1−M−N4	−	−	96.3(12)	97.7(11)	98.17(15)
M−O1−H1	−	−	−	−	99(4)
O1−H1−O2	−	−	−	−	168(5)
M−C1−C2−O2	−	−	−	−	−72(3)
C1−M−C3	−	89.9(4)	−	−	−
C2−M−C4	−	84.4(4)	−	−	−
C1−C2−M	72.1(7)	69.5(4)	−	−	−
C3−C4−M	72.1(6)	70.7(5)	−	−	−
C4−C3−M	69.2(6)	72.3(5)	−	−	−

cedure was applied to account for the electron density of the solvent molecule.

8aBPh$_4$: The five-membered dioxolane ring has the envelope form and occurs in two conformations. As expected there is considerable positional overlap for some of the atoms (C1A and C1B, C2A and C2B, O1A and O1B). Therefore, some geometrical constraints had to be applied: the two conformations were 'SAMEd' and the anisotropic thermal displacement parameters were tied. Calculations (PLATON, Spek 1995)[33] showed two distinct voids, one of 229 Å^3, containing 68 electrons, around a two-fold axis (position 4e, 0, *y*, 1/4; *y* = −0.036), and one of 152 Å^3, containing 44 electrons, around an inversion center (position 4b: 1/2, 0, 0). Based on the synthetic route and evidence from NMR spectroscopy, it is assumed that these electron densities represent one molecule of diethyl ether ($C_4H_{10}O$, 42 electrons) plus one molecule of acetonitrile (CH_3CN, 22 electrons) in the first void (64 electrons, 28.5 Å^3/atom), and one molecule of dichloroethane ($C_2H_4Cl_2$, 50 electrons) in the second void (30.2 Å^3/atom). It was not possible to assign any physically meaningful parameters to the electron densities found in the difference fourier map. Therefore the SQUEEZE procedure was applied to account for these electron densities.

9aBPh$_4$: Hydrogen atom H1 was clearly visually observed in a difference fourier map and its position was subsequently determined automatically. Its positional and thermal parameters were refined freely and this refinement proved to be stable. The position of H1 is well outside the regions influenced by the SQUEEZE procedure described later on.

From the anisotropic thermal displacement parameters for C2 and O2 it is clear that these atoms show a large positional disorder. Although it is possible to use several partially occupied positions for these atoms, no physically reasonable models result from these parameters, at least not any better than the model presented here. Splitting up these atoms serves no other purpose but to lower the *R*-value. The calculated hydrogen positions on C2 are therefore merely indications of possible positions.

Calculations (PLATON, Spek 1995)[33] showed two distinct voids, one of 239 Å^3, containing 58 electrons, around a two-fold axis (position 4e, 0, *y*, 1/4; *y* = −0.041), and one of 152 Å^3, containing 39 electrons, around an inversion center (position 4b: 1/2, 0, 0). Based on the synthetic route and evidence from NMR spectroscopy, it is assumed that these electron densities possibly represent one molecule of diethyl ether ($C_4H_{10}O$, 42 electrons) plus one molecule of acetonitrile (CH_3CN, 22 electrons) in the first void (64 electrons, 29.9 Å^3/non-hydrogen atom), and one molecule of dichloroethane ($C_2H_4Cl_2$, 50 electrons) in the second void (38.0 Å^3/non-hydrogen atom). These assumptions are in accordance with the earlier crystal structure determination of the original crystal of **8a**BPh$_4$ before its exposure to glass-filtered daylight, and account for the calculated physical molecular properties as reported in this paper.

It was not possible to assign any physically meaningful parameters to the electron densities found in the difference fourier map. Therefore, the SQUEEZE procedure was applied to account for these electron densities.

CCDC-187013 (**3**PF$_6$), CCDC-187012 (**5**PF$_6$), CCDC-157414 (**8a**BPh$_4$), and CCDC-170096 (**9a**BPh$_4$) contain the supplementary crystallographic data for this paper. These data can be obtained free of charge at www.ccdc.cam.ac.uk/conts/retrieving.html [or from the Cambridge Crystallographic Data Centre, 12, Union Road, Cambridge CB2 1EZ, UK; Fax: (internat.) +44−1223/336-033; E-mail: deposit@ccdc.cam.ac.uk].

Synthesis

Bis(ethene)[*N*-(2-pyridylmethyl)-*N*,*N*-bis(2-pyridylmethyl-κ*N*)amine-κ*N*]iridium(I) Hexafluorophosphate (3PF$_6$): Ethene was bubbled through a solution of $[(C_8H_{14})_2IrCl]_2$ (325 mg, 0.36 mmol) in MeOH (13 mL) until a clear solution was obtained. Under an ethene atmosphere, tpa (216 mg, 0.74 mmol) was added and the reaction mixture was stirred for 10 minutes. KPF$_6$ (167 mg, 0.91 mmol) was then added under an ethene atmosphere, and after stirring for 1 hour, the solution was cooled to −78 °C. The cold suspension was filtered under a nitrogen atmosphere and the white

Table 5. Crystallographic data

	3^+	5^+	$8a^+$	$9a^+$
Empirical formula	$C_{22}H_{26}F_6IrN_4P$	$C_{47}H_{54}BN_4ORh$	$C_{48}H_{50.50}BClN_{4.50}O_{2.50}Rh$	$C_{48}H_{50.50}BClN_{4.50}O_{2.50}Rh$
Crystal color	Light yellow transparent	Transparent yellow-brown	Transparent yellow	Transparent yellow
Crystal shape	Regular platelet	Irregular fragment	Irregular fragment	Irregular fragment
Crystal size [mm]	0.53 × 0.46 × 0.10	0.36 × 0.24 × 0.10	0.29 × 0.22 × 0.13	0.29 × 0.22 × 0.13
Molecular weight	683.64	804.66	879.60	879.60
T [K]	208(2)	208(2)	150(2)	150(2)
Crystal system	Monoclinic	Monoclinic	Monoclinic	Monoclinic
Space group	P 21/c	P 21/n	C 2/c	C 2/c
Unit cell dim. from N refl.	23	21	17718	14986
a [Å]	7.538(2)	11.555(2)	35.8688(5)	36.0362(2)
b [Å]	14.831(3)	17.523(5)	10.7328(2)	10.77600(10)
c [Å]	20.753(10)	19.686(5)	24.2609(4)	24.2975(2)
α [°]	90	90	90	90
β [°]	90.07(3)	97.38(2)	116.6660(10)	116.3883(4)
γ [°]	90	90	90	90
V [Å^3]	2320.2(13)	3952.9(17)	8346.4(2)	8452.21(11)
$\rho_{calcd.}$ [g·cm^{-3}]	1.957	1.352	1.400	1.382
Z	4	4	8	8
Diffractometer	Enraf−Nonius CAD4	Enraf−Nonius CAD4	Nonius Kappa CCD with rotating anode	Nonius Kappa CCD with rotating anode
Abs. Coefficient [mm^{-1}]	5.890	3.805	0.520	0.514
Scan	ω-2θ	ω-2θ	Area detector, and ω scan	Area detector, and ω scan
Radiation (graphite mon.)	Mo-K_α	Cu-Kα	Mo-K_α	Mo-K_α
Wavelength [Å]	0.71073	1.54184	0.71073	0.71073
F(000)	1328	1688	3656	3656
Θ range [°]	2.70−27.48	3.39−69.93	1.27−27.48	1.73−25.35
Index ranges	$-9 \le h \le 0$ $-19 \le k \le 0$ $-26 \le l \le 26$	$0 \le h \le 14$ $0 \le k \le 21$ $-23 \le l \le 23$	$-46 \le h \le 46$ $-13 \le k \le 13$ $-31 \le l \le 31$	$-43 \le h \le 43$ $-12 \le k \le 12$ $-29 \le l \le 29$
Abs. Corr.	Semi-empir. Ψ-scan[a]	Semi-empir. Ψ-scan[a]	None	None
Range of rel. transm. fac.	4.786, 0.696	1.083, 0.947	−	−
Measured reflections	5707	7865	17718	14986
Unique reflections	5314	7478	9548	7719
[R_{int}]	[0.0481]	[0.0633]	[0.0508]	[0.0294]
Observed reflections [$I_0 > 2\sigma(I_0)$]	4542	4765	5801	5510
Data/restraints/parameters	5314/0/308	7478/0/485	9548/184/506	7719/0/473
Goodness-of-fit on F^2	1.090	1.004	0.963	1.054
SHELXL-97 weight parameters	0.1169, 42.6696	0.0970, 0.0000	0.0586, 0.0000	0.0870, 6.0419
Final $R1$, $wR2$ [$I > 2\sigma(I)$]	0.0657, 0.1843	0.0702, 0.1617	0.0459, 0.1080	0.0494, 0.1402
$R1$, $wR2$ [all data]	0.0766, 0.1992	0.1140, 0.1815	0.0904, 0.1186	0.0721, 0.1492
Diff. Peak and hole [e·Å^{-3}]	6.907, −3.638	1.635, −1.208	0.770, −0.508	0.899, −0.643

[a] A. C. T. North, D. C. Philips, F. S. Mathews, *Acta Crystallogr.* **1968**, *A24*, 351−359.

residue was washed with MeOH (3 × 1 mL) and dried in vacuo. Complex **3**PF_6 was obtained as a white powder. Yield: 290 mg (58%). ^1H NMR (200 MHz, CD_2Cl_2, 300 K): δ = 8.69 (ddd, $^3J_{H,H}$ = 4.9, $^4J_{H,H}$ = 1.8, $^5J_{H,H}$ = 0.9 Hz, 1 H, Py_a-H6), 7.80 (dt, $^3J_{H,H}$ = 7.7, $^4J_{H,H}$ = 1.9 Hz, 1 H, Py_a-H4), 7.73 (dt, $^3J_{H,H}$ = 7.8, $^4J_{H,H}$ = 1.6 Hz, 2 H, Py_b-H4), 7.60 (d, $^3J_{H,H}$ = 4.9 Hz, 2 H, Py_b-H6), 7.37 (m, 3 H, Py-H3), 7.14 (t, $^3J_{H,H}$ = 7.0 Hz, 3 H, Py-H5), 5.50 (d[AB], $^2J_{H,H}$ = 15.4 Hz, 2 H, NCH_2Py_b), 4.65 (d[AB], $^2J_{H,H}$ = 15.6 Hz, 2 H, NCH_2Py_b), 4.39 (s, 2 H, NCH_2Py_a), 3.36 (br.t, $^3J_{H,H}$ = 9.4 Hz, 2 H, CH_2CH_2), 3.22 (t, $^3J_{H,H}$ = 9.7 Hz, 2 H, CH_2CH_2), 1.94 (t, $^3J_{H,H}$ = 9.8 Hz, 2 H, CH_2CH_2), 1.85 (br.t, $^3J_{H,H}$ = 9.7 Hz, 2 H, CH_2CH_2) ppm; $^{13}C\{^1H\}$ NMR (125 MHz, CD_3CN, 243 K): δ = 166.2 (Py_b-C2), 154.6 (Py_a-C2), 150.8 (Py_a-C6), 150.4 (Py_b-C6), 138.8(Py_b-C4), 138.2 (Py_a-C4), 127.2 (Py_a-C3/5), 126.6 (Py_b-C3/5), 124.8 (Py_b-C3/5), 124.5 (Py_a-C3/5), 65.4 (NCH_2Py_b), 65.3 (NCH_2Py_a), 39.8 (br., CH_2CH_2), 37.3 (br., CH_2CH_2), 34.8 (CH_2CH_2), 30.3 (CH_2CH_2) ppm; elemental analysis for **3**PF_6 ($C_{22}H_{26}F_6IrN_4P$; 683.66): calcd. C 38.65, H 3.83, N 8.20; found C 38.78, H 3.90, N 8.36 %.

Bis(ethene)[*N*-(2-pyridylmethyl)-*N*,*N*-bis(2-pyridylmethyl-κ*N*)amine-κ*N*]iridium(I) Tetraphenylborate (3BPh$_4$): Complex **3**BPh_4 was obtained by the same procedure as **3**PF_6, using $NaBPh_4$ instead of KPF_6.

(Ethene)[*N*,*N*,*N*-tris(2-pyridylmethyl-κ*N*)amine-κ*N*]-iridium(I) Hexafluorophosphate (4PF$_6$): Complex **4**PF_6 was synthesized according to the same procedure as bis(ethene) complex **3**PF_6, but nitrogen was bubbled through the MeOH solution before the addition of KPF_6. Complex **4**PF_6 was obtained as a yellow/orange powder. Yield: 83%. ^1H NMR (200 MHz, CD_3CN, 300 K): δ = 9.19 (d, $^3J_{H,H}$ = 5.2 Hz, 1 H, Py_a-H6), 8.28 (d, $^3J_{H,H}$ = 5.3 Hz, 2 H, Py_b-H6), 7.64 (t, $^3J_{H,H}$ = 7.8 Hz, 3 H, Py-H4), 7.21 (m, 4 H, Py-H3 and Py_a-H5), 7.05 (t, $^3J_{H,H}$ = 6.6 Hz, 2 H, Py_b-H5), 5.11 (d[AB], $^2J_{H,H}$ = 15.3 Hz, 2 H, NCH_2Py_b), 4.83 (d[AB], $^2J_{H,H}$ =

15.3 Hz, 2 H, NCH_2Py$_b$), 4.69 (s, 2 H, NCH_2Py$_a$), 1.28 (m, 4 H, CH_2CH_2) ppm; ^{13}C{^{1}H} NMR (75 MHz, CD$_3$CN, 300 K): δ = 165.5 (Py$_b$-C2), 161.1 (Py$_a$-C2), 152.4 (Py$_a$-C6), 151.4 (Py$_b$-C6), 137.8 (Py$_a$-C4), 136.3 (Py$_b$-C4), 125.8 (Py$_b$-C3/5), 124.6 (Py$_a$-C3/5), 123.4 (Py$_b$-C3/5), 122.3 (Py$_a$-C3/5), 71.6 (NCH$_2$Py$_b$), 65.9 (NCH$_2$Py$_a$), 4.3 (CH$_2$CH$_2$), 4.1 (CH$_2$$CH_2$) ppm. ESI-MS (THF): 511 [M − PF$_6$]$^+$, 483 [M − CH$_2$CH$_2$ − PF$_6$]$^+$; elemental analysis for **4**PF$_6$ (C$_{20}$H$_{22}$F$_6$IrN$_4$P; 655.61): calcd. C 36.64, H 3.38, N 8.55; found C 36.63, H 3.44, N 8.66 %.

(Ethene)[*N*,*N*,*N*-tris(2-pyridylmethyl-κ*N*)amine-κ*N*]iridium(I) Tetraphenylborate (4BPh$_4$): Complex **4**BPh$_4$ was obtained by the same procedure as **4**PF$_6$, using NaBPh$_4$ instead of KPF$_6$.

Bis(ethene){3,11-dimethyl-3,11,17,18-tetraazatricyclo[11.3.1.1^{5,9}]octadeca-1(17),5(18),6,8,13,15-hexaene-κ^4*N^1*,*N^2*,*N^3*}rhodium(I) Hexafluorophosphate (5PF$_6$): [Rh(μ-Cl)(C$_2$H$_4$)$_2$]$_2$ (100 mg, 0.26 mmol) was added to a suspension of NaHCO$_3$ (100 mg, 1.2 mmol) in methanol (5 mL) at −20 °C. The reaction mixture was stirred for 15 minutes, after which N$_4$Me$_2$ (138 mg, 0.51 mmol) was added. After stirring for 5 minutes at −20 °C, the reaction mixture was cooled to −78 °C and stirred for 30 minutes. Undissolved material was removed by filtration. A solution of KPF$_6$ (100 mg, 0.54 mmol) in methanol (1 mL) was then added to the filtrate at −78 °C, causing the precipitation of a light yellow solid. After stirring for 1 hour, the solid was collected by filtration. Additional KPF$_6$ (60 mg, 0.33 mmol) was added to the filtrate. The solution was warmed to room temperature for two minutes, after which it was cooled to −78 °C again. This produced a second batch of solid, which was collected by filtration after stirring for 15 minutes. The combined solids were washed with methanol and dried under vacuum. Yield: 245 mg (83%). ^{1}H NMR (500 MHz, [D$_6$]acetone, 203 K): δ = 7.73 (t, $^3J_{H,H}$ = 7.8 Hz, 2 H, Py-H4), 7.37 (d, $^3J_{H,H}$ = 7.5 Hz, 2 H, Py-H3/5), 7.28 (d, $^3J_{H,H}$ = 7.8 Hz, 2 H, Py-H3/5), 6.06 (d[AB], $^2J_{H,H}$ = 14.1 Hz, 2 H, NCH_2Py), 5.17 (d[AB], $^2J_{H,H}$ = 16.7 Hz, 2 H, NCH_2Py), 4.51 (d[AB], $^2J_{H,H}$ = 16.9 Hz, 2 H, NCH_2Py), 4.46 (d[AB], $^2J_{H,H}$ = 14.1 Hz, 2 H, NCH_2Py), 3.84 (s, 3 H, NCH_3), 3.22 (m, 2 H, CH_2CH$_2$), 2.92 (br.t, $^3J_{H,H}$ = 10.3 Hz, 2 H, CH$_2$CH_2), 2.53 (br.t, $^3J_{H,H}$ = 10.9 Hz, 2 H, CH_2CH_2), 2.25 (s, 3 H, NCH_3), 1.72 (m, 2 H, CH_2CH$_2$) ppm; ^{13}C{^{1}H} NMR (100 MHz, [D$_6$]acetone, 243 K): δ = 160.0 (Py-C2/6), 158.1 (Py-C2/6), 138.4 (Py-C4), 126.3 (Py-C3/5), 121.9 (Py-C3/5), 68.1 (NCH$_2$Py), 65.4 (NCH$_2$Py), 57.7 (br., CH$_2$$CH_2$), 52.6 (N$CH_3$), 46.6 (br., CH$_2$$CH_2$), 37.7 (N$CH_3$) ppm. ESI-MS (CH$_3$CN): 427 [M − PF$_6$]$^+$, 399 [M − (CH$_2CH_2$) − PF$_6$]$^+$.

(Ethene){3,11-dimethyl-3,11,17,18-tetraazatricyclo[11.3.1.1^{5,9}]octadeca-1(17),5(18),6,8,13,15-hexaene-κ^4*N^1*,*N^2*,*N^3*,*N^4*}rhodium(I) Hexafluorophosphate (6PF$_6$): After stirring **5**PF$_6$ (245 mg, 0.43 mmol) in [D$_6$]acetone (10 mL) for 4 hours, diethyl ether (40 mL) was added. A red solid precipitated and was collected by filtration and washed with diethyl ether. The obtained brick-red solid was isolated by filtration, washed with diethyl ether and dried in vacuo. Yield 112 mg (48%). ^{1}H NMR (200 MHz, CD$_3$CN, 298 K): δ = 7.62 (t, $^3J_{H,H}$ = 7.9 Hz, 2 H, Py-H4), 7.11 (d, $^3J_{H,H}$ = 7.8 Hz, 4 H, Py-H3 and Py-H5), 4.01 (d[AB], $^2J_{H,H}$ = 15.1 Hz, 4 H, NCH_2Py), 3.82 (d[AB], $^2J_{H,H}$ = 15.0 Hz, 4 H, NCH_2Py), 2.54 (d, $^2J_{H,Rh}$ = 2.4 Hz, 4 H, CH_2CH_2), 2.15 (d, $^3J_{H,Rh}$ = 1.3 Hz, 6 H, NCH_3) ppm; ^{13}C{^{1}H} NMR (75 MHz, [D$_6$]acetone, 297 K): δ = 155.4 (Py-C2 and Py-C6), 136.6 (Py-C4), 121.3 (Py-C3 and Py-C5), 76.1 (NCH$_2$Py), 49.8 (NCH$_3$), 24.8 (d, $J_{C,Rh}$ = 18 Hz, CH$_2$$CH_2$) ppm. ESI-MS (CH$_3$CN): 399 [M − PF$_6$]$^+$, 371 [M − (CH$_2CH_2$) − PF$_6$]$^+$.

(2-Peroxyethyl-κ^2*C^1*,*O^2*)[*N*,*N*,*N*-tris(2-pyridylmethyl-κ*N*)amine-κ*N*]rhodium(III) Tetraphenylborate (8aBPh$_4$): Compound **7**BPh$_4$ was ground with a mortar and exposed to air at room temperature and was left in the dark for 2 days at atmospheric pressure.[11] **8a**BPh$_4$ was obtained in > 90% yield, as determined by ^{1}H NMR spectroscopy. Crystals obtained from a 1,2-dichloroethane solution proved to be unsuitable for X-ray diffraction. However, the crystals obtained were used for elemental analysis. Both ^{1}H NMR spectroscopy and elemental analysis of these crystals showed that they contained 1.5 molecules of 1,2-dichloroethane per cation. ^{1}H NMR (300 MHz, CD$_3$CN, 297 K): δ = 8.75 (d, $^3J_{H,H}$ = 5.4 Hz, 1 H, Py$_a$-H6), 8.66 (d, $^3J_{H,H}$ = 5.5 Hz, 2 H, Py$_b$-H6), 7.81 (dt, $^3J_{H,H}$ = 7.8, $^4J_{H,H}$ = 1.7 Hz, 2 H, Py$_b$-H4), 7.69 (dt, $^3J_{H,H}$ = 7.8, $^4J_{H,H}$ = 1.7 Hz, 1 H, Py$_a$-H4), 7.40 (d, $^3J_{H,H}$ = 8.0 Hz, 2 H, Py$_b$-H3), 7.35 (m, 3 H, Py$_a$-H5 and Py$_b$-H5), 7.28 (m, 8 H, BAr-H2), 7.16 (dt, $^3J_{H,H}$ = 7.8, $^4J_{H,H}$ = 0.9 Hz, 1 H, Py$_a$-H3), 6.99 (t, $^3J_{H,H}$ = 7.4 Hz, 8 H, BAr-H3), 6.84 (t, $^3J_{H,H}$ = 7.3 Hz, 4 H, BAr-H4), 4.88 (d[AB], $^2J_{H,H}$ = 15.6 Hz, 2 H, NCH_2Py$_b$), 4.71 (d[AB], $^2J_{H,H}$ = 15.1 Hz, 2 H, NCH_2Py$_b$), 4.57 (s, 2 H, NCH_2Py$_a$), 3.25 (t, $^3J_{H,H}$ = 6.1 Hz, 2 H, RhCH$_2$CH_2OO), 2.57 (dt, $^3J_{H,H}$ = 6.1, $^2J_{H,Rh}$ = 2.4 Hz, 2 H, RhCH_2CH$_2$OO) ppm; ^{13}C{^{1}H} NMR (75 MHz, CD$_3$CN, 297 K): δ = 164.6 (q, $^1J_{C,B}$ = 49.5 Hz, BAr-C1), 162.7 (Py$_b$-C2), 158.6 (Py$_a$-C2), 150.1 (Py$_b$-C6), 149.5 (Py$_a$-C6), 139.4 (Py$_a$-C4), 139.3 (Py$_b$-C4), 136.5 (BAr-C2), 126.4 (q, $^3J_{C,B}$ = 2.8 Hz, BAr-C3), 125.5 (Py$_b$-C3), 125.4 (Py$_a$-C3), 124.2 (Py$_b$-C5), 122.6 (BAr-C4), 121.9 (Py$_a$-C5), 72.9 (NCH$_2$Py$_a$), 70.2 (N-CH$_2$-Py$_b$ and RhCH$_2$$CH_2$OO), 35.0 (d, $^1J_{C,Rh}$ = 25.0 Hz, RhCH$_2$CH$_2$OO) ppm. ESI-MS (CD$_3$CN): 453 [M − BPh$_4$]$^+$, 425 [M − CH$_2$CH$_2$ − BPh$_4$]$^+$, 409 [M − C$_2$H$_4$O − BPh$_4$]$^+$, 393 [M − C$_2$H$_4$O$_2$ − BPh$_4$]$^+$, 391 [M − C$_2$H$_4$O$_2$ − H$_2$ − BPh$_4$]$^+$; elemental analysis for **8a**BPh$_4$·1^1/$_2$C$_2$H$_4$Cl$_2$ (C$_{47}$H$_{48}$BCl$_3$N$_4$O$_2$Rh; 921.00): calcd. C 61.36, H 5.26, N 6.09; found C 61.36, H 5.44, N 6.17 %.

(2-Peroxyethyl-κ^2*C^1*,*O^2*)[*N*,*N*,*N*-tris(2-pyridylmethyl-κ*N*)amine-κ*N*]rhodium(III) Hexafluorophosphate (8aPF$_6$/8bPF$_6$): Complex **7**PF$_6$ was ground with a mortar and exposed to air at room temperature and was left in the dark for 2 days at atmospheric pressure.[11] A mixture of **8a**PF$_6$ and **8b**PF$_6$ in an approximate ratio of 1:1 was obtained in > 90% yield, as determined by ^{1}H NMR spectroscopy. The data for **8b**PF$_6$ are given: ^{1}H NMR (500 MHz, CD$_3$CN, 298 K): δ = 8.86 (d, $^3J_{H,H}$ = 5.4 Hz, 1 H, Py$_a$-H6), 8.56 (d, $^3J_{H,H}$ = 5.4 Hz, 2 H, Py$_b$-H6), 7.83 (dt, $^3J_{H,H}$ = 7.8, $^4J_{H,H}$ = 1.4 Hz, 2 H, Py$_b$-H4),7.63 (t, $^3J_{H,H}$ = 7.3 Hz, 1 H, Py$_a$-H4), 7.48 (d, $^3J_{H,H}$ = 7.8 Hz, 2 H, Py$_b$-H3), 7.35 (t, $^3J_{H,H}$ = 6.6 Hz, 2 H, Py$_b$-H5), 7.25 (m, 1 H, Py$_a$-H5), 7.14 (d, $^3J_{H,H}$ = 7.8 Hz, 1 H, Py$_a$-H3), 5.12 (d[AB], $^2J_{H,H}$ = 15.6 Hz, 2 H, NCH_2Py$_b$), 5.00 (d[AB], $^2J_{H,H}$ = 15.6 Hz, 2 H, NCH_2Py$_b$), 4.80 (s, 2 H, NCH_2Py$_a$), 3.55 (dt, $^3J_{H,H}$ = 6.1, $^2J_{H,Rh}$ = 2.4 Hz, 2 H, RhCH_2CH$_2$OO), 3.41 (t, $^3J_{H,H}$ = 6.1 Hz, 2 H, RhCH$_2$CH_2OO) ppm; ^{13}C{^{1}H} NMR (50 MHz, CD$_3$CN, 300 K): δ = 164.6 (Py$_b$-C2), 162.7 (Py$_a$-C6), 152.5 (Py$_a$-C6), 150.5 (Py$_b$-C6), 139.7 (Py$_b$-C4), 138.7 (Py$_a$-C4), 125.9 (Py$_b$-C3), 125.5 (Py$_a$-C3), 124.6 (Py$_b$-C5), 122.6 (Py$_a$-C5), 72.8 (RhCH$_2$$CH_2$OO), 67.9 (N$CH_2Py_b$), 65.4 (N$CH_2Py_a$), 44.8 (d, $^1J_{C,Rh}$ = 28.8 Hz, RhCH$_2$CH$_2$OO) ppm. ESI-MS (CD$_3$CN): 453 [M − PF$_6$]$^+$, 425 [M − CH$_2$CH$_2$ − PF$_6$]$^+$, 409 [M − C$_2$H$_4$O − PF$_6$]$^+$, 393 [M − C$_2$H$_4$O$_2$ − PF$_6$]$^+$, 391 [M − C$_2$H$_4$O$_2$ −H$_2$ − PF$_6$]$^+$.

(2-Peroxyethyl-κ^2*C^1*,*O^2*)[*N*,*N*,*N*-tris(2-pyridylmethyl-κ*N*)amine-κ*N*]iridium(III) Tetraphenylborate (10aBPh$_4$): Compound **4**BPh$_4$ was ground with a mortar and exposed to air for 5 days. **10a**BPh$_4$ was obtained in > 90% yield, as determined by ^{1}H NMR spectroscopy.[11] ^{1}H NMR (500 MHz, CD$_3$CN, 243 K): δ = 8.67 (m, 3 H, Py-H6), 7.77 (dt, $^3J_{H,H}$ = 7.8, $^4J_{H,H}$ = 1.6 Hz, 2 H, Py$_b$-H4), 7.68 (dt, $^3J_{H,H}$ = 7.8, $^4J_{H,H}$ = 1.6 Hz, 1 H, Py$_a$-H4), 7.38 (d, $^3J_{H,H}$ = 7.7 Hz, 2 H, Py$_b$-H3), 7.30 (m, 3 H, Py-H5), 7.26 (m, 8 H, BAr-H2), 7.16 (d, $^3J_{H,H}$ = 7.7 Hz, 1 H, Py$_a$-H3), 6.98 (t, $^3J_{H,H}$ =

7.5 Hz, 8 H, BAr-H3), 6.82 (t, $^3J_{H,H}$ = 7.3 Hz, 4 H, BAr-H4), 4.92 (d[AB], $^2J_{H,H}$ = 15.4 Hz, 2 H, NC*H*$_2$Py$_b$), 4.67 (d[AB], $^2J_{H,H}$ = 15.4 Hz, 2 H, NC*H*$_2$Py$_b$), 4.56 (s, 2 H, NC*H*$_2$Py$_a$), 2.54 (t, $^3J_{H,H}$ = 6.2 Hz, 2 H, RhCH$_2$C*H*$_2$OO), 2.03 (t, $^3J_{H,H}$ = 6.2 Hz, 2 H, RhC*H*$_2$CH$_2$OO) ppm; ^{13}C{^{1}H} NMR (125 MHz, CD$_3$CN, 243 K): δ = 164.8 (Py$_b$-C2), 163.9 (q, ^1J (C,B)= 49.2 Hz, BAr-C1), 159.3 (Py$_a$-C2), 149.0 (Py$_b$-C6), 148.1 (Py$_a$-C6), 138.5 (Py$_a$-C4), 138.0 (Py$_b$-C4), 135.8 (q, $^2J_{C,B}$ = 1.3 Hz, BAr-C2), 126.1 (q, $^3J_{C,B}$ = 2.9 Hz, BAr-C3), 124.9 (Py$_b$-C3/5 and Py$_a$-C3/5), 123.9 (Py$_b$-C3/5), 122.1 (BAr-C4), 121.3 (Py$_a$-C3/5), 72.1 (N*C*H$_2$Py$_b$), 71.8 (N*C*H$_2$Py$_\alpha$ or IrCH$_2$*C*H$_2$OO), 71.1 (N*C*H$_2$Py$_\alpha$ or IrCH$_2$*C*H$_2$OO), 15.8 (Ir*C*H$_2$CH$_2$OO) ppm.

(2-Peroxyethyl-κ^2*C^1*,*O^2*)[*N*,*N*,*N*-tris(2-pyridylmethyl-κ*N*)-amine-κ*N*]iridium(III) Hexafluorophosphate (10aPF$_6$/10bPF$_6$): Compound **4**PF$_6$ was ground with a mortar and exposed to air for 5 days.[11] A mixture of the isomeric 3-irida-1,2-dioxolanes **10a**PF$_6$ and **10b**PF$_6$ in an approximate ratio of 2:5 was formed in > 90% yield, as determined by ^{1}H NMR spectroscopy. The data for **10b**PF$_6$ are given: ^{1}H NMR (500 MHz, CD$_3$CN, 243 K): δ = 8.93 (d, $^3J_{H,H}$ = 5.5 Hz, 1 H, Py$_a$-H6), 8.58 (d, $^3J_{H,H}$ = 5.13 Hz, 2 H, Py$_b$-H6), 7.75 (dt, $^3J_{H,H}$ = 7.8, $^4J_{H,H}$ = 1.3 Hz, 2 H, Py$_b$-H4), 7.56 (dt, $^3J_{H,H}$ = 7.8, $^4J_{H,H}$ = 1.3 Hz, 1 H, Py$_a$-H4), 7.42 (d, $^3J_{H,H}$ = 8.1 Hz, 2 H, Py$_b$-H3), 7.27 (t, $^3J_{H,H}$ = 6.2 Hz, 2 H, Py$_b$-H5), 7.15 (m, 2 H, Py$_a$-H5 and Py$_a$-H3), 5.04 (d[AB], $^2J_{H,H}$ = 15.4 Hz, 2 H, NC*H*$_2$Py$_b$), 4.94 (d[AB], $^2J_{H,H}$ = 15.8 Hz, 2 H, NC*H*$_2$Py$_b$), 4.76 (s, 2 H, NC*H*$_2$Py$_a$), 2.69 (t, $^3J_{H,H}$ = 6.7 Hz, 2 H, IrC*H*$_2$CH$_2$OO), 2.63 (t, $^3J_{H,H}$ = 6.7 Hz, 2 H, IrCH$_2$C*H*$_2$OO) ppm. ^{13}C NMR (125 MHz, CD$_3$CN, 243 K): δ = 165.9 (Py$_b$-C2), 162.6 (Py$_a$-C2), 152.4 (Py$_a$-C6), 149.5 (Py$_b$-C6), 138.7 (Py$_b$-C4), 137.3 (Py$_a$-C4), 125.3 (Py$_b$-C3/5), 125.1 (Py$_a$-C3/5), 124.2 (Py$_b$-C3/5), 121.8 (Py$_a$-C3/5), 71.6 (IrCH$_2$*C*H$_2$OO), 69.2 (N*C*H$_2$Py$_b$), 66.4 (N*C*H$_2$Py$_a$), 23.9 (Ir*C*H$_2$-CH$_2$OO) ppm.

(2-Peroxyethyl-κ^2*C^1*,*O^2*){3,11-dimethyl-3,11,17,18-tetraazatricyclo[11.3.1.1^{5,9}]octadeca-1(17),5(18),6,8,13,15-hexaene-κ^4*N^1*,*N^2*,*N^3*,*N^4*}rhodium(III) Hexafluorophosphate (16PF$_6$): Complex **6**PF$_6$ was exposed to an oxygen atmosphere at room temperature for 5 days at atmospheric pressure.[11] The color changed from red to yellow ochre. ^{1}H NMR (200 MHz, CD$_3$CN, 298 K): δ = 7.75 (t, $^3J_{H,H}$ = 7.9 Hz, 1 H, Py-H4), 7.66 (t, $^3J_{H,H}$ = 7.9 Hz, 1 H, Py-H4), 7.28 (d, $^3J_{H,H}$ = 7.8 Hz, 2 H, Py-H3/5), 7.14 (d, $^3J_{H,H}$ = 7.8 Hz, 2 H, Py-H3/5), 4.57 (d[AB], $^2J_{H,H}$ = 15.3 Hz, 2 H, NC*H*$_2$Py), 4.36 (d[AB], $^2J_{H,H}$ = 16.6 Hz, 2 H, NC*H*$_2$Py), 4.16 (d[AB], $^2J_{H,H}$ = 15.2 Hz, 4 H, NC*H*$_2$Py), 3.66 (dt, $^3J_{H,H}$ = 6.4, $^3J_{H,Rh}$ = 0.7 Hz, 2 H, RhCH$_2$C*H*$_2$OO), 2.90 (dt, $^3J_{H,H}$ = 6.5, $^2J_{H,Rh}$ = 2.5 Hz, 2 H, RhC*H*$_2$CH$_2$OO), 2.71 (d, $^3J_{H,Rh}$ = 1.2 Hz, 6 H, NC*H*$_3$) ppm; ^{13}C{^{1}H} NMR (125 MHz, CD$_3$CN, 243 K): δ = 157.0 (Py-C2/6), 155.0 (Py-C2/6), 139.3 (Py-C4), 138.2 (Py-C4), 121.6 (Py-C3/5), 120.8 (Py-C3/5), 74.4 (N*C*H$_2$Py), 72.5 (N*C*H$_2$Py), 71.7 (RhCH$_2$*C*H$_2$OO), 50.1 (N*C*H$_3$), 30.3 (d, $J_{C,Rh}$ = 25 Hz, Rh*C*H$_2$CH$_2$OO) ppm. ESI-MS (CH$_3$CN): 431 [M − PF$_6$]$^+$.

(Formylmethyl-κ*C^1*)(hydroxy)[*N*,*N*,*N*-tris(2-pyridylmethyl-κ*N*)amine-κ*N*]rhodium(III) Tetraphenylborate (9aBPh$_4$). Method A: A stirred solution of **8a**BPh$_4$ in CD$_3$CN under nitrogen was exposed to the glass-filtered light of a high pressure mercury vapor lamp[34] for 90 minutes at −30 °C. **9a**BPh$_4$ was obtained in > 90% yield, as determined by ^{1}H NMR spectroscopy.

Method B: HBAr$^F_4$ (5.5 mg, 5.4 µmol) was added to a solution of **8a**BPh$_4$ (41.8 mg, 54 µmol) in CD$_3$CN (1 mL) under N$_2$. **9a**BPh$_4$ was obtained in approximately 70% yield in approximately 1 hour, as determined by ^{1}H NMR spectroscopy. ^{1}H NMR (200 MHz, CD$_3$CN, 300 K): δ = 9.26 (t, $^3J_{H,H}$ = 5.0 Hz, 1 H, RhCH$_2$C*H*O), 9.21 (br.d, $^3J_{H,H}$ = 6.0 Hz, 1 H, Py$_a$-H6), 8.62 (br.d, $^3J_{H,H}$ = 5.6 Hz, 2 H, Py$_b$-H6), 7.84 (dt, $^3J_{H,H}$ = 7.8, $^4J_{H,H}$ = 1.6 Hz, 2 H, Py$_b$-H4), 7.73 (dt, $^3J_{H,H}$ = 7.8, $^4J_{H,H}$ = 1.6 Hz, 1 H, Py$_a$-H4), 7.32 (m, 6 H, Py-H3 and Py-H5), 7.27 (m, 8 H, BAr-H2), 6.99 (t, $^3J_{H,H}$ = 7.4 Hz, 8 H, BAr-H3), 6.83 (t, $^3J_{H,H}$ = 7.2 Hz, 4 H, BAr-H4), 5.01 (d[AB], $^2J_{H,H}$ = 15.9 Hz, 2 H, NC*H*$_2$Py$_b$), 4.71 (d[AB], $^2J_{H,H}$ = 14.9 Hz, NC*H*$_2$Py$_b$), 4.67 (s, 2 H, NC*H*$_2$Py$_a$), 2.69 (dd, $^3J_{H,H}$ = 5.1, $^2J_{H,Rh}$ = 2.9 Hz, 2 H, RhC*H*$_2$CHO) ppm; ^{13}C{^{1}H} NMR (125 MHz, CD$_3$CN, 243 K): δ = 209.0 (RhCH$_2$*C*HO), 163.9 (q, $^1J_{C,B}$ = 49.2 Hz, BAr-C1), 162.4 (Py$_b$-C2), 159.0 (Py$_a$-C2), 149.9 (Py$_b$-C6), 147.2 (Py$_a$-C6), 139.3 (Py$_b$-C4), 139.2 (Py$_a$-C4), 135.7 (BAr-C2), 126.1 (q, $^3J_{C,B}$ = 2.7 Hz, BAr-C3), 125.4 (Py$_b$-C5/C3), 124.9 (Py$_a$-C5/C3), 124.4 (Py$_b$-C5/C3), 122.1 (BAr-C4), 121.2 (Py$_a$-C5/C3), 70.7 (N*C*H$_2$Py$_a$), 68.3 (N*C*H$_2$Py$_b$), 26.9 (d, $^1J_{C,Rh}$ = 21.0 Hz, Rh*C*H$_2$CHO) ppm. ESI-MS (CD$_3$CN): 453 [M − BPh$_4$]$^+$, 435 [M − H$_2$O − BPh$_4$]$^+$, 425 [M − C$_2$H$_4$ − BPh$_4$]$^+$, 409 [M − C$_2$H$_4$O − BPh$_4$]$^+$, 393 [M − C$_2$H$_4$O$_2$ − BPh$_4$]$^+$, 391 [M − C$_2$H$_4$O$_2$ − H$_2$ − BPh$_4$]$^+$. IR (KBr): $\tilde{\nu}$ = 1655 cm^{-1}.

(Formylmethyl-κ*C^1*)(hydroxy)-[*N*,*N*,*N*-tris(2-pyridylmethyl-κ*N*)amine-κ*N*]rhodium(III) Hexafluorophosphate (9aPF$_6$/9bPF$_6$): *Solid* **8a**PF$_6$/**8b**PF$_6$ was exposed to a N$_2$ atmosphere saturated with H$_2$O for three days at room temperature. A mixture of **9a**PF$_6$ and **9b**PF$_6$ in an approximate ratio of 1:1 was obtained in > 90% yield, according to ^{1}H NMR spectroscopy. The data for **9b**PF$_6$ are given: ^{1}H NMR (500 MHz, CD$_3$CN, 243 K): δ = 9.98 (t, $^3J_{H,H}$ = 4.9 Hz, 1 H, RhCH$_2$C*H*O), 8.68 (d, $^3J_{H,H}$ = 5.5 Hz, 2 H, Py$_b$-H6), 8.53 (d, $^3J_{H,H}$ = 5.5 Hz, 1 H, Py$_a$-H6), 7.84 (m, 2 H, Py$_b$-H4), 7.66 (dt, $^3J_{H,H}$ = 7.7, $^4J_{H,H}$ = 1.5 Hz, 1 H, Py$_a$-H4), 7.48 (d, $^3J_{H,H}$ = 8.2 Hz, 2 H, Py$_b$-H3), 7.36 (t, $^3J_{H,H}$ = 6.6 Hz, 2 H, Py$_b$-H5), 7.28 (t, $^3J_{H,H}$ = 6.6 Hz, 1 H, Py$_a$-H5), 7.17 (d, $^3J_{H,H}$ = 8.8 Hz, 1 H, Py$_a$-H3), 5.39 (d[AB], $^2J_{H,H}$ = 15.0 Hz, 2 H, NC*H*$_2$Py$_b$), 4.88 (s, 2 H, NC*H*$_2$Py$_a$), 4.76 (d[AB], $^2J_{H,H}$ = 15.0 Hz, 2 H, NC*H*$_2$Py$_b$), 3.47 (dd, $^3J_{H,H}$ = 4.8, $^2J_{H,Rh}$ = 2.9 Hz, 2 H, RhC*H*$_2$CHO) ppm; ^{13}C{^{1}H} NMR (125 MHz, CD$_3$CN, 243 K): δ = 210.8 (d, $^2J_{C,Rh}$ = 9.6 Hz, RhCH$_2$*C*HO), 165.0 (Py$_b$-C2), 163.5 (Py$_a$-C2), 151.5 (Py$_b$-C6), 150.2 (Py$_a$-C6), 139.6 (Py$_b$-C4), 138.8 (Py$_a$-C4), 125.4 (Py$_b$-C5/C3), 125.1 (Py$_a$-C5/C3), 124.4 (Py$_b$-C5/C3), 122.1 (Py$_a$-C5/C3), 66.4 (N*C*H$_2$Py$_b$), 66.2 (N*C*H$_2$Py$_a$), 34.5 (d, $^1J_{C,Rh}$ = 25.0 Hz, Rh*C*H$_2$CHO) ppm. ESI-MS (CH$_3$CN): 453 [M − PF$_6$]$^+$.

(Formylmethyl-κ*C^1*)(aqua)[*N*,*N*,*N*-tris(2-pyridylmethyl-κ*N*)-amine-κ*N*]rhodium(III) Tetraphenylborate Tetra[3,5-bis(trifluoromethyl)phenyl]borate (20a[BPh$_4$][BAr$^F{}_4$]): HBAr$^F_4$ (57 mg, 0.11 mmol) was added to a solution of **8a**BPh$_4$ (40 mg, 0.1 mmol) in CD$_3$CN (1.0 mL) under N$_2$. **20a**(BPh$_4$)(BAr$^F_4$) was obtained in approximately 85% yield, as determined by ^{1}H NMR spectroscopy. ^{1}H NMR (200 MHz, CD$_3$CN, 300 K): δ = 9.51 (t, $^3J_{H,H}$ = 4.8 Hz, 1 H, RhCH$_2$C*H*O), 8.96 (d, $^3J_{H,H}$ = 5.5 Hz, 1 H, Py$_a$-H6), 8.52 (d, $^3J_{H,H}$ = 5.7 Hz, 2 H, Py$_b$-H6), 7.95 (dt, $^3J_{H,H}$ = 7.8, $^4J_{H,H}$ = 1.6 Hz, Py$_b$-H4), 7.81 (dt, $^3J_{H,H}$ = 7.8, $^4J_{H,H}$ = 1.6 Hz, Py$_a$-H4),7.73 (m, 8 H, BAr$^F_4$-H2), 7.68 (s, 4 H, BAr$^F_4$-H4), 7.6−7.4 (m, 5 H, Py$_b$-H3, Py$_b$-H5 and Py$_a$-H3/5), 7.33 (m, 8 H, BAr-H2), 7.21 (m, 1 H, Py$_a$-H3/5), 7.01 (t, $^3J_{H,H}$ = 7.4 Hz, 8 H, BAr-H3), 6.85 (t, $^3J_{H,H}$ = 6.9 Hz, 4 H, BAr-H4), 5.15 (d[AB], $^2J_{H,H}$ = 16.4 Hz, 2 H, NC*H*$_2$Py$_b$), 4.82 (s, 2 H, NC*H*$_2$Py$_a$), 4.69 (d[AB], $^2J_{H,H}$ = 16.6 Hz, 2 H, NC*H*$_2$Py$_b$), 3.05 (dd, $^3J_{H,H}$ = 4.9, $^2J_{H,Rh}$ = 2.7 Hz, 2 H, RhC*H*$_2$CHO) ppm; ^{13}C{^{1}H} NMR (125 MHz, CD$_3$CN, 243 K): δ = 206.7 (d, $^2J_{C,Rh}$ = 1.9 Hz, RhCH$_2$*C*HO), 164.0 (q, $^1J_{C,B}$ = 49.2 Hz, BAr-C1), 161.9 (q, $^1J_{C,B}$ = 49.8 Hz, BAr^F-C1), 161.6 (Py$_b$-C2), 158.0 (Py$_a$-C2), 151.5 (Py$_b$-C6), 148.7 (Py$_a$-C6), 140.9 (Py$_b$-C4), 140.4 (Py$_a$-C4), 135.8 (BAr-C2), 134.9 (BAr^F-C2), 129.0 (qq, $^2J_{C,F}$ = 31.4, $^3J_{C,B}$ = 2.9 Hz, BAr^F-C3), 126.4 (Py$_b$-C5/C3), 126.2 (q, $^3J_{C,B}$ = 2.6 Hz, BAr-C3), 125.8 (Py$_a$-C5/C3), 125.4 (Py$_b$-C5/C3), 124.6 (q, $^1J_{C,F}$ = 271.9 Hz, BAr^F-CF$_3$), 122.3 (BAr-C4), 122.1 (Py$_a$-C5/C3), 73.5 (N*C*H$_2$Py$_a$), 69.6 (N*C*H$_2$Py$_b$), 27.8 (d, $^1J_{C,Rh}$ =

20.4 Hz, Rh*C*H$_2$CHO) ppm. (The signal for BAr$^{\mathrm{F}}$-C4 is obscured by one of the solvent signals). ESI-MS (CH$_3$CN): 227 [M − BPh$_4$ − BAr$^{\mathrm{F}}_4$]$^{2+}$, 218 [M − H$_2$O − BPh$_4$ − BAr$^{\mathrm{F}}_4$]$^{2+}$.

(Formylmethyl-κ*C*^{1})(hydroxy)[*N*,*N*,*N*-tris(2-pyridylmethyl-κ*N*)amine-κ*N*]iridium(III) Tetraphenylborate (11aBPh$_4$): A solution of **10a**BPh$_4$ (85.2 mg, 99 μmol) in CH$_3$CN (1 mL) was stirred at room temperature. After 4 hours, diethyl ether was added and a yellow solid precipitated. After filtration, the solid was washed with diethyl ether and dried in vacuo. Yield: 49.1 mg (58%). ^{1}H NMR (500 MHz, CD$_3$CN, 298 K): δ = 9.25 (br.d, $^3J_{\mathrm{H,H}}$ = 5.7 Hz, 1 H, Py$_a$-H6), 9.21 (t, $^3J_{\mathrm{H,H}}$ = 5.1 Hz, 1 H, IrCH$_2$C*H*O), 8.71 (d, $^3J_{\mathrm{H,H}}$ = 5.7 Hz, 2 H, Py$_b$-H6), 7.78 (dt, $^3J_{\mathrm{H,H}}$ = 7.8, $^4J_{\mathrm{H,H}}$ = 1.5 Hz, 2 H, Py$_b$-H4), 7.68 (dt, $^3J_{\mathrm{H,H}}$ = 7.8, $^4J_{\mathrm{H,H}}$ = 1.6 Hz, 1 H, Py$_a$-H4), 7.4−7.1 (m, 6 H, Py-H3 and Py-H5), 7.29 (m, 8 H, BAr-H2), 7.00 (t, $^3J_{\mathrm{H,H}}$ = 7.4 Hz, 8 H, BAr-H3), 6.84 (t, $^3J_{\mathrm{H,H}}$ = 7.2 Hz, 4 H, BAr-H4), 4.86 (s, 2 H, NC*H*$_2$Py$_b$), 4.85 (s, 2 H, NC*H*$_2$Py$_b$), 4.56 (s, 2 H, NC*H*$_2$Py$_a$), 3.07 (d, $^3J_{\mathrm{H,H}}$ = 5.3 Hz, 2 H, IrC*H*$_2$CHO) ppm; ^{13}C{^{1}H} NMR (125 MHz, CD$_3$CN, 298 K): δ = 209.4 (IrCH$_2$*C*HO), 165.8 (Py$_b$ -C2), 164.6 (q, ^1J (C,B)= 49.3 Hz, BAr-C1), 160.8 (Py$_a$-C2), 149.7 (Py$_b$-C6), 146.3 (Py$_a$-C6), 139.2 (Py$_a$-C4), 139.0 (Py$_b$-C4), 136.5 (BAr-C2), 126.4 (q, $^3J_{\mathrm{C,B}}$ = 2.8 Hz, BAr-C3), 125.7 (Py$_b$-C3/5), 125.1 (Py$_a$-C3/5), 124.7 (Py$_b$-C3/5), 122.6 (BAr-C4), 121.5 (Py$_a$-C3/5), 72.9 (N*C*H$_2$Py$_a$), 71.4 (N*C*H$_2$Py$_b$), 16.3 (Ir*C*H$_2$CHO) ppm. ESI-MS (CH$_3$CN): 543 [M − BPh$_4$]$^+$, 525 [M − H$_2$O − BPh$_4$]$^+$, 499 [M − C$_2$H$_4$O − BPh$_4$]$^+$, 483 [M − C$_2$H$_4$O$_2$ − BPh$_4$]$^+$, 391 [M − CH$_2$C$_5$H$_4$N − H$_4$O$_2$ − BPh$_4$]$^+$. IR (KBr): ṽ = 1654 cm^{-1}.

(Formylmethyl-κ*C*^{1})(hydroxy)[*N*,*N*,*N*-tris(2-pyridylmethyl-κ*N*)amine-κ*N*]iridium(III) Hexafluorophosphate (11aPF$_6$/11bPF$_6$): **11a**PF$_6$/**11b**PF$_6$ was prepared by a procedure similar to that of **11a**BPh$_4$, using **10a**PF$_6$/**10b**PF$_6$ instead of **10a**BPh$_4$. Yield: 93%. ^{1}H NMR (500 MHz, CD$_3$CN, 298 K): δ = 10.11 (t, $^3J_{\mathrm{H,H}}$ = 5.0 Hz, 1 H, IrCH$_2$C*H*O), 8.73 (d, $^3J_{\mathrm{H,H}}$ = 5.9 Hz, 3 H, Py-H6), 7.81 (dt, $^3J_{\mathrm{H,H}}$ = 7.7, $^4J_{\mathrm{H,H}}$ = 1.5 Hz, 2 H, Py$_b$-H4), 7.61 (dt, $^3J_{\mathrm{H,H}}$ = 7.7, $^4J_{\mathrm{H,H}}$ = 1.5 Hz, 1 H, Py$_a$-H4), 7.48 (d, $^3J_{\mathrm{H,H}}$ = 8.1 Hz, 2 H, Py$_b$-H3), 7.30 (t, $^3J_{\mathrm{H,H}}$ = 6.4 Hz, 2 H, Py$_b$-H5), 7.23 (t, $^3J_{\mathrm{H,H}}$ = 6.8 Hz, 1 H, Py$_a$-H5), 7.17 (d, $^3J_{\mathrm{H,H}}$ = 7.7 Hz, 1 H, Py$_a$-H3), 5.40 (d, $^2J_{\mathrm{H,H}}$ = 15.0 Hz, 2 H, NC*H*$_2$Py$_b$), 4.82 (s, 2 H, NC*H*$_2$Py$_a$), 4.77 (d, $^2J_{\mathrm{H,H}}$ = 14.7 Hz, 2 H, NC*H*$_2$Py$_b$), 3.66 (d, $^3J_{\mathrm{H,H}}$ = 4.8 Hz, 2 H, IrC*H*$_2$CHO) ppm; ^{13}C{^{1}H} NMR (125 MHz, CD$_3$CN, 300 K): δ = 211.2 (IrCH$_2$*C*HO), 167.1 (Py$_b$-C2), 164.9 (Py$_a$-C2), 152.0 (Py$_b$-C6), 151.1 (Py$_a$-C6), 139.5 (Py$_b$-C4), 138.4 (Py$_a$-C4), 125.9 (Py$_b$-C3/5), 125.7 (Py$_a$-C3/5), 124.5 (Py$_b$-C3/5), 122.2 (Py$_a$-C3/5), 69.3 (N*C*H$_2$Py$_a$), 68.6 (N*C*H$_2$Py$_b$), 20.7 (Ir*C*H$_2$CHO) ppm. ESI-MS (CH$_3$CN): 543 [M − PF$_6$]$^+$, 541 [M − H$_2$ − PF$_6$]$^+$.

(Formylmethyl-κ*C*^{1})(hydroxy){3,11-dimethyl-3,11,17,18-tetraazatricyclo[11.3.1.1^{5,9}]octadeca-1(17),5(18),6,8,13,15-hexaene-κ^4*N*^{1},*N*^{2},*N*^{3},*N*^{4}}rhodium(III) Hexafluorophosphate (17PF$_6$): *Solid* **16**PF$_6$ was put under a nitrogen atmosphere saturated with H$_2$O vapor for 4 days. The product was dried in vacuo. ^{1}H NMR (400 MHz, CD$_3$CN, 297 K): δ = 9.57 (t, $^3J_{\mathrm{H,H}}$ = 5.4 Hz, 1 H, C*H*O), 7.77 (t, $^3J_{\mathrm{H,H}}$ = 7.8 Hz, 1 H, Py-H4), 7.66 (t, $^3J_{\mathrm{H,H}}$ = 8.0 Hz, 1 H, Py-H4), 7.29 (d, $^3J_{\mathrm{H,H}}$ = 8.0 Hz, 2 H, Py-H3/5), 7.18 (d, $^3J_{\mathrm{H,H}}$ = 8.0 Hz, 2 H, Py-H3/5), 4.76 (d[AB], $^2J_{\mathrm{H,H}}$ = 16.5 Hz, 2 H, NC*H*$_2$Py), 4.51 (d[AB], $^2J_{\mathrm{H,H}}$ = 16.5 Hz, 2 H, NC*H*$_2$Py), 4.30 (d[AB], $^2J_{\mathrm{H,H}}$ = 16.5 Hz, 2 H, NC*H*$_2$Py), 4.29 (d[AB], $^2J_{\mathrm{H,H}}$ = 15.9 Hz, 2 H, NC*H*$_2$Py), 3.14 (dd, $^3J_{\mathrm{H,H}}$ = 5.3, $^3J_{\mathrm{H,Rh}}$ = 3.2 Hz, 1 H, RhC*H*$_2$CHO), 2.95 (s, 6 H, NC*H*$_3$) ppm; ^{13}C{^{1}H} NMR (125 MHz, CD$_3$CN, 243 K): δ = 207.7 (RhCH$_2$*C*HO), 157.4 (Py-C2/6), 155.7 Py-C2/6), 139.9 (Py-C4), 138.7 (Py-C4), 121.4 (Py-C3/5), 74.7 (N*C*H$_2$Py), 72.6 (N*C*H$_2$Py), 50.8 (N*C*H$_3$), 33.4 (d, $^1J_{\mathrm{C,Rh}}$ = 21.2 Hz, Rh*C*H$_2$CHO) ppm. FAB-MS (NPOE, CH$_3$CN): 431 [M − PF$_6$]$^+$. ESI-MS (CH$_3$CN): 431 [M − PF$_6$]$^+$, 413 [M − H$_2$O − PF$_6$]$^+$, 287 [M − C$_2$H$_4$O − PF$_6$]$^+$, 371 [M − C$_2$H$_4$O$_2$ − PF$_6$]$^+$, 369 [M − C$_2$H$_4$O$_2$ − H$_2$ − PF$_6$]$^+$. IR (CD$_3$CN): ṽ = 1651 cm^{-1}.

(Formylmethyl-κ*C*^{1})(hydrogen carbonate)[*N*,*N*,*N*-tris(2-pyridylmethyl-κ*N*)amine-κ*N*]rhodium(III) Tetraphenylborate (21aBPh$_4$): A solution of **9a**BPh$_4$ was left standing under a CO$_2$ atmosphere. **21a**BPh$_4$ was formed within 5 minutes in a quantitative yield, according to ^{1}H NMR spectroscopy. Isolation of **21a**BPh$_4$ was not possible, since the insertion of CO$_2$ is a reversible reaction. Precipitation and filtration led to the isolation of **9a**BPh$_4$. ^{1}H NMR (200 MHz, CD$_3$CN, 298 K): δ = 9.53 (t, $^3J_{\mathrm{H,H}}$ = 4.6 Hz, 1 H, RhCH$_2$C*H*O), 8.99 (d, $^3J_{\mathrm{H,H}}$ = 4.8 Hz, 1 H, Py$_a$-H6), 8.86 (d, $^3J_{\mathrm{H,H}}$ = 5.8 Hz, 2 H, Py$_b$-H6), 7.85 (dt, $^3J_{\mathrm{H,H}}$ = 7.8, $^4J_{\mathrm{H,H}}$ = 1.6 Hz, 2 H, Py$_b$-H4), 7.73 (dt, $^3J_{\mathrm{H,H}}$ = 7.7, $^4J_{\mathrm{H,H}}$ = 1.6 Hz, 1 H, Py$_a$-H4), 7.5−7.2 (m, 5 H, Py-H5 and Py$_b$-H3), 7.29 (m, 8 H, BAr-H2), 7.15 (d, $^3J_{\mathrm{H,H}}$ = 7.9 Hz, 1 H, Py$_a$-H3), 6.99 (t, $^3J_{\mathrm{H,H}}$ = 7.4 Hz, 8 H, BAr-H3), 6.84 (t, $^3J_{\mathrm{H,H}}$ = 7.2 Hz, 4 H, BAr-H4), 4.99 (d[AB], $^2J_{\mathrm{H,H}}$ = 16.2 Hz, 2 H, NC*H*$_2$Py$_b$), 4.58 (s, 2 H, NC*H*$_2$Py$_a$), 4.50 (d[AB], $^2J_{\mathrm{H,H}}$ = 15.8 Hz, 2 H, NC*H*$_2$Py$_b$), 3.23 (dd, $^3J_{\mathrm{H,H}}$ = 4.8, $^2J_{\mathrm{H,Rh}}$ = 2.5 Hz, 2 H, RhC*H*$_2$CHO) ppm; ^{13}C{^{1}H} NMR (50 MHz, CD$_3$CN): δ = 210.1 (RhCH$_2$*C*HO), 164.6 (q, $^1J_{\mathrm{C,B}}$ = 49.3 Hz, BAr-C1), 162.3 (Py$_b$-C2), 158.4 (Py$_a$-C2), 152.2 (Py$_b$-C6), 148.4 (Py$_a$-C6), 140.4 (Py$_b$-C4), 140.1 (Py$_a$-C4), 136.5 (BAr-C2), 126.40 (q, $^3J_{\mathrm{C,B}}$ = 2.6 Hz, BAr-C3), 125.9 (Py$_b$-C3/5), 125.5 (CO$_2$), 124.9 (Py$_b$-C3/5), 122.6 (BAr-C4), 121.9 (Py$_a$-C3/5), 73.2 (N*C*H$_2$Py$_a$), 70.0 (N*C*H$_2$Py$_b$), 28.1 (d, $^1J_{\mathrm{C,Rh}}$ = 20.7 Hz, Rh*C*H$_2$CHO) ppm. (The signal for Py$_a$-C3/5 is obscured by one of the other signals). IR (CD$_3$CN): ṽ = 1694, 1664 cm^{-1}.

(Formylmethyl-κ*C*^{1})(hydrogen carbonate)[*N*,*N*,*N*-tris(2-pyridylmethyl-κ*N*)amine-κ*N*]iridium(III) Tetraphenylborate (22aBPh$_4$): **22a**BPh$_4$ was prepared by a procedure similar to that of **21a**BPh$_4$, using **11a**BPh$_4$ instead of **9a**BPh$_4$. Complex **22a**BPh$_4$ was also obtained in a quantitative yield, according to ^{1}H NMR spectroscopy, but could not be isolated. ^{1}H NMR (500 MHz, CD$_3$CN, 298 K): δ = 9.46 (t, $^3J_{\mathrm{H,H}}$ = 4.8 Hz, 1 H, IrCH$_2$C*H*O), 9.02 (d, $^3J_{\mathrm{H,H}}$ = 5.5 Hz, 1 H, Py$_a$-H6), 8.95 (d, $^3J_{\mathrm{H,H}}$ = 5.5 Hz, 2 H, Py$_b$-H6), 7.82 (dt, $^3J_{\mathrm{H,H}}$ = 7.9, $^4J_{\mathrm{H,H}}$ = 1.5 Hz, 2 H, Py$_b$-H4), 7.71 (dt, $^3J_{\mathrm{H,H}}$ = 7.7, $^4J_{\mathrm{H,H}}$ = 1.5 Hz, 1 H, Py$_a$-H4), 7.44 (d, $^3J_{\mathrm{H,H}}$ = 7.7 Hz, 2 H, Py$_b$-H3), 7.40 (t, $^3J_{\mathrm{H,H}}$ = 6.6 Hz, 1 H, Py$_a$-H5), 7.33 (t, $^3J_{\mathrm{H,H}}$ = 6.6 Hz, 2 H, Py$_b$-H5), 7.29 (m, 8 H, BAr-H2), 7.18 (d, $^3J_{\mathrm{H,H}}$ = 8.0 Hz, 1 H, Py$_a$-H3), 6.99 (t, $^3J_{\mathrm{H,H}}$ = 7.3 Hz, 8 H, BAr-H3), 6.84 (t, $^3J_{\mathrm{H,H}}$ = 7.1 Hz, 4 H, BAr-H4), 4.93 (d[AB], $^2J_{\mathrm{H,H}}$ = 15.3 Hz, 2 H, NC*H*$_2$Py$_b$), 4.75 (d[AB], $^2J_{\mathrm{H,H}}$ = 15.7 Hz, 2 H, NC*H*$_2$Py$_b$), 4.55 (s, 2 H, NC*H*$_2$Py$_a$), 3.39 (d, $^3J_{\mathrm{H,H}}$ = 4.8 Hz, 2 H, IrC*H*$_2$CHO) ppm; ^{13}C{^{1}H} NMR (125 MHz, CD$_3$CN, 298 K): δ = 211.1 (IrCH$_2$*C*HO), 164.6 (q, ^1J (C,B)= 49.4 Hz, BAr-C1), 164.5 (Py$_b$ -C2), 159.9 (Py$_a$-C2), 152.4 (Py$_b$-C6), 147.9 (Py$_a$-C6), 139.8 (Py$_a$-C4), 139.7 (Py$_b$-C4), 136.5 (BAr-C2), 126.4 (q, $^3J_{\mathrm{C,B}}$ = 2.8 Hz, BAr-C3), 125.9 (Py$_b$-C3/5), 125.6 (Py$_b$-C3/5), 124.7 (Py$_a$-C3/5), 122.6 (BAr-C4), 121.8 (Py$_a$-C3/5), 74.9 (N*C*H$_2$Py$_a$), 72.1 (N*C*H$_2$Py$_b$), 14.8 (Ir*C*H$_2$CHO) ppm. ESI-MS (CO$_2$ saturated CH$_3$CN): 587 [M − BPh$_4$]$^+$, 543 [M − CO$_2$ − BPh$_4$]$^+$. IR (CH$_3$CN): ṽ = 1663, 1635 cm^{-1}.

(Propene)[*N*,*N*,*N*-tris(2-pyridylmethyl-κ*N*)amine-κ*N*]rhodium(I) Tetraphenylborate (23BPh$_4$): Propene was bubbled through a solution of [(ethene)$_2$RhCl]$_2$ (54 mg, 0.14 mmol) and NaHCO$_3$ (50 mg) in MeOH (3 mL) at room temperature for 30 minutes. Tpa (81 mg, 0.28 mmol) was then added, and the reaction mixture was stirred for 1 hour. After filtration the residue was washed with methanol (2 × 0.25 mL) and NaBPh$_4$ (85.5 mg, 0.25 mmol) was added to the filtrate. The reaction mixture was stirred for 1 hour, filtered, washed with MeOH (3 × 1 mL) and dried in vacuo. Yield: 130 mg (69%). ^{1}H NMR (200 MHz, [D$_6$]acetone, 300 K): δ = 9.39 (d, $^{3}J_{H,H}$ = 4.7 Hz, 1 H, Py-H6), 8.33 (d, $^{3}J_{H,H}$ = 5.5 Hz, 1 H, Py-H6), 8.03 (d, $^{3}J_{H,H}$ = 5.3 Hz, 1 H, Py-H6), 7.67 (m, 3 H, Py-H4), 7.35 (m, 11 H, BAr-H2 and Py-H3/5), 7.17 (m, 3 H, Py-H3/5), 6.92 (t, $^{3}J_{H,H}$ = 7.2 Hz, 8 H, BAr-H3), 6.77 (t, $^{3}J_{H,H}$ = 6.9 Hz, 4 H, BAr-H4), 5.68 (d[AB], $^{2}J_{H,H}$ = 15.1 Hz, 1 H, NCH_2Py), 5.57 (d[AB], $^{2}J_{H,H}$ = 15.1 Hz, 1 H, NCH_2Py), 4.93 (d[AB], $^{2}J_{H,H}$ = 15.3 Hz, 1 H, NCH_2Py), 4.92 (d[AB], $^{2}J_{H,H}$ = 15.5 Hz, 1 H, NCH_2Py), 4.63 (s, 2 H, NCH_2Py), 2.47 (m, 1 H, CH$_2$CHCH$_3$), 2.28 (dm, $^{3}J_{H,H}$ = 7.8 Hz, 1 H, CH_2CHCH$_3$), 1.93 (dm, $^{3}J_{H,H}$ = 9.8 Hz, 1 H, CH_2CHCH$_3$), 0.87 (dd, $^{3}J_{H,H}$ = 6.2, $^{2}J_{H,Rh}$ = 1.3 Hz, 3 H, CH$_2$CHCH_3) ppm; ^{13}C{^{1}H} NMR (100 MHz, [D$_6$]acetone, 297 K): δ = 165.0 (q, $^{1}J_{C,B}$ = 49.7 Hz, BAr-C1), 164.1 (Py-C2), 163.5 (Py-C2), 159.3 (Py-C2), 152.4 (Py-C6), 151.9 (Py-C6), 151.2 (Py-C6), 138.3 (Py-C4), 137.5 (Py-C4), 137.4 (Py-C4), 137.1 (BAr-C2), 126.1 (m, BAr-C3), 125.5 (Py-C3/5), 125.2 (Py-C3/5), 124.7 (Py-C3/5), 123.7 (Py-C3/5), 123.4 (Py-C3/5), 122.4 (Py-C3/5), 122.4 (BAr-C4), 70.1 (NCH$_2$Py), 69.9 (NCH$_2$Py), 64.6 (NCH$_2$Py), 40.3 (d, $^{1}J_{C,Rh}$ = 19.7 Hz, CH$_2$CHCH$_3$/CH$_2$$CHCH_3$), 33.8 (d, $^{1}J_{C,Rh}$ = 19.8 Hz, CH$_2$CHCH$_3$/CH$_2$$CHCH_3$), 20.6 (CH$_2CHCH_3$) ppm. ESI-MS (acetone): 435 [M − BPh$_4$], 393 [M − C$_3$H$_6$ − BPh$_4$], 301 [M − C$_3$H$_6$ − CH$_2$C$_5$H$_4$N − BPh$_4$].

(Peroxo-κ^2*O^1*,*O^2*)[*N*,*N*,*N*-tris(2-pyridylmethyl-κ*N*)amine-κ*N*]rhodium(III) Tetraphenylborate (24BPh$_4$): Complex **23**BPh$_4$ was exposed to air for 3 days. **24**BPh$_4$ was obtained in > 90% yield, as determined by ^{1}H NMR spectroscopy. ^{1}H NMR (500 MHz, CD$_3$CN, 233 K): δ = 9.23 (d, $^{3}J_{H,H}$ = 5.5 Hz, 1 H, Py$_a$-H6), 8.37 (d, $^{3}J_{H,H}$ = 5.1 Hz, 2 H, Py$_b$-H6), 7.77 (dt, $^{3}J_{H,H}$ = 7.8, $^{4}J_{H,H}$ = 1.6 Hz, 2 H, Py$_b$-H4), 7.65 (dt, $^{3}J_{H,H}$ = 7.8, $^{4}J_{H,H}$ = 1.6 Hz, 1 H, Py$_a$-H4), 7.34 (d, $^{3}J_{H,H}$ = 7.7 Hz, 2 H, Py$_b$-H3), 7.28 (m, 11 H, BAr-H2, Py-H5), 7.12 (d, $^{3}J_{H,H}$ = 7.7 Hz, 1 H, Py$_a$-H3), 6.98 (t, $^{3}J_{H,H}$ = 7.3 Hz, 8 H, BAr-H3), 6.81 (t, $^{3}J_{H,H}$ = 7.2 Hz, 4 H, BAr-H4), 5.21 (d[AB], $^{2}J_{H,H}$ = 16.1 Hz, 2 H, NCH_2Py$_b$), 4.82 (d[AB], $^{2}J_{H,H}$ = 16.1 Hz, 2 H, NCH_2Py$_b$), 4.53 (s, 2 H, NCH_2Py$_a$) ppm; ^{13}C{^{1}H} NMR (125 MHz, CD$_3$CN, 233 K): δ = 163.8 (q, $^{1}J_{C,B}$ = 49.2 Hz, BAr-C1), 162.8 (Py$_b$-C2), 159.8 (Py$_a$-C2), 152.5 (Py$_a$-C6), 150.1 (Py$_b$-C6), 139.4 (Py$_b$-C4), 139.1 (Py$_a$-C4), 135.6 (BAr-C2), 126.0 (q, $^{3}J_{C,B}$ = 2.7 Hz, BAr-C3), 125.4 (Py$_b$-C3/5), 123.4 (Py$_b$-C3/5), 122.1 (BAr-C4), 121.8 (Py$_a$-C3/5), 70.4 (NCH$_2$Py$_b$), 67.6 (NCH$_2$Py$_a$) ppm. (The signal for Py$_a$-C3/5 is obscured by one of the other signals). ESI-MS (CH$_3$CN): 425 [M − BPh$_4$]$^+$, 393 [M − O$_2$ − BPh$_4$]$^+$, (467 [?]$^+$ [22]).

(Hydroperoxy)(hydroxy)[*N*,*N*,*N*-tris(2-pyridylmethyl-κ*N*)amine-κ*N*]rhodium(III) Tetraphenylborate (25BPh$_4$): Complex **24**BPh$_4$ was exposed to a N$_2$ atmosphere saturated with water for 3 days. **25**BPh$_4$ was obtained in > 90% yield, as determined by ^{1}H NMR spectroscopy. ^{1}H NMR (200 MHz, CD$_3$CN, 300 K): δ = 8.76 (d, $^{3}J_{H,H}$ = 5.9 Hz, 1 H, Py$_a$-H6), 8.70 (d, $^{3}J_{H,H}$ = 5.7 Hz, 2 H, Py$_b$-H6), 7.86 (dt, $^{3}J_{H,H}$ = 7.8, $^{4}J_{H,H}$ = 1.6 Hz, 2 H, Py$_b$-H4), 7.69 (dt, $^{3}J_{H,H}$ = 7.8, $^{4}J_{H,H}$ = 1.7 Hz, 1 H, Py$_a$-H4), 7.5−7.3 (m, 5 H, Py$_b$-H3 and Py-H5), 7.28 (m, 8 H, BAr-H2), 7.11 (d, $^{3}J_{H,H}$ = 7.8 Hz, 1 H, Py$_a$-H3), 6.99 (t, $^{3}J_{H,H}$ = 7.3 Hz, 8 H, BAr-H3), 6.83 (t, $^{3}J_{H,H}$ = 7.0 Hz, 4 H, BAr-H4), 5.35 (d[AB], $^{2}J_{H,H}$ = 15.5 Hz, 2 H, NCH_2Py$_b$), 4.75 (m, 4 H, NCH_2Py$_b$ and NCH_2Py$_a$) ppm. ESI-MS (CH$_3$CN): 443 [M − BPh$_4$]$^+$, 425 [M − H$_2$O − BPh$_4$]$^+$, 410 [M − HO$_2$ − BPh$_4$]$^+$, 393 [M − OH − O$_2$H − BPh$_4$]$^+$, 300 [M − CH$_2$C$_5$H$_4$N − O$_2$H − H$_2$O − BPh$_4$]$^+$.

Acknowledgments

This work was supported by the Netherlands Organization for Scientific Research (NWO-CW). We thank Johnson Matthey Ltd. for a generous loan of RhCl$_3$·3H$_2$O. S. Thewissen, P. M. van Galen, and H. I. V. Amatdjais-Groenen are gratefully acknowledged for the ESI-MS measurements. Prof. Dr. P. Chen from the ETH Zürich is kindly acknowledged for allowing us to use the Finnigan TSQ 7000 mass spectrometer. Prof. Dr. Hans-Jörg Krüger (Universität Kaiserslautern, Germany) is kindly acknowledged for providing us with details on the synthesis of N$_4$Me$_2$.

---

[1] [1a] H. Mimoun, M. M. P. Machirant, I. Seree de Roch, *J. Am. Chem. Soc.* **1978**, *100(17)*, 5437−5444. [1b] G. Read, *J. Mol. Catal.* **1988**, *44*, 15−33. [1c] M. Bressan, F. Morandini, A. Morvillo, P. Rigo, *J. Organomet. Chem.* **1985**, *280*, 139−146. [1d] R. A. Sheldon, J. A. van Doorn, *J. Organomet. Chem.* **1975**, *94*, 115−129. [1e] H. Mimoun, *Angew. Chem.* **1982**, *21*, 734; *Angew. Chem. Int. Ed. Engl.* **1982**, *94*, 750−766. [1f] H. Mimoun, I. Seree de Roch, L. Sajus, *Tetrahedron* **1970**, *26*, 37−50.

[2] D. V. Deubel, J. Sundermeyer, G. Frenking, *J. Am. Chem. Soc.* **2000**, *122*, 10101−10108.

[3] [3a] G. Read, M. Urgelles, A. M. R. Galas, M. B. Hursthouse, *J. Chem. Soc., Dalton Trans.* **1983**, 911−913. [3b] L. Pandolfo, G. Paiaro, G. Valle, P. Ganis, *Gazz. Chim. Ital.* **1985**, *115*, 59−63.

[4] [4a] M. Krom, R. G. E. Coumans, J. M. M. Smits, A. W. Gal, *Angew. Chem.* **2001**, *113*, 2164−2166; *Angew. Chem. Int. Ed.* **2001**, *40(11)*, 2106−2108. [4b] M. Krom, R. G. E. Coumans, J. M. M. Smits, A. W. Gal, *Angew. Chem.* **2002**, *114*, 595−599; *Angew. Chem. Int. Ed.* **2002**, *41(4)*, 575−579.

[5] B. de Bruin, M. J. Boerakker, J. A. W. Verhagen, R. de Gelder, J. M. M. Smits, A. W. Gal, *Chem. Eur. J.* **2000**, *6*, 298−312.

[6] [6a] B. de Bruin, J. A. Brands, J. J. J. M. Donners, M. P. J. Donners, R. de Gelder, J. M. M. Smits, A. W. Gal, A. L. Spek, *Chem. Eur. J.* **1999**, *5*, 2921−2936. [6b] B. de Bruin, R. J. N. A. M. Kicken, N. F. A. Suos, M. P. J. Donners, C. J. den Reijer, A. J. Sandee, R. de Gelder, J. M. M. Smits, A. W. Gal, A. L. Spek, *Eur. J. Inorg. Chem.* **1999**, 1581−1592. [6c] B. de Bruin, Th. P. J. Peters, J. B. M. Wilting, S. Thewissen, J. M. M. Smits, A. W. Gal, *Eur. J. Inorg. Chem.* **2002**, 2671.

[7] The X-ray structures of three other iridium bis(ethene) complexes stabilized by tridentate nitrogen donor ligands have been reported: [7a] Y. Alvarado, O. Boutry, E. Gutiérrez, A. Monge, M. C. Nicasio, M. L. Poveda, P. J. Pérez, C. Ruíz, C. Bianchini, E. Carmona, *Chem. Eur. J.* **1997**, *3*, 860−873. [7b] J. S. Wiley, W. J. Oldham, Jr., D. M. Heinekey, *Organometallics* **2000**, *19*, 1670−1676. The third complex is stabilized by a tpa-type ligand.[6c]

[8] *N*,*N′*-Dimethyl-2,11-diaza[3,3](2,6)pyridinophane = 3,11-dimethyl-3,11,17,18-tetraazatricyclo[11.3.1.1^{5,9}]octadeca-1(17),5(18),6,8,13,15-hexaene.

[9] [9a] H. Kelm, H. J. Kruger, *Eur. J. Inorg. Chem.* **1998**, 1381−1385. [9b] T. Sciarone, J. Hoogboom, P. P. J. Schlebos, P. H. M. Budzelaar, R. de Gelder, J. M. M. Smits, A. W. Gal, *Eur. J. Inorg. Chem.* **2002**, 457−464. [9c] S. Plentz Meneghetti, P. J. Lutz, J. Kress, *Organometallics* **2001**, *20*, 5050−5055.

[10] [10a] H. Sakaba, C. Kabuto, H. Horino, M. Arai, *Bull. Chem. Soc. Jpn.* **1990**, *63*, 1822−1824. [10b] H. Kelm, H. J. Kruger, *Inorg. Chem.* **1996**, *35*, 3533−3540. [10c] W. O. Koch, V. Schunemann, M. Gerdan, A. X. Trautwein, H. J. Kruger, *Chem. Eur. J.* **1998**, *4(7)*, 1255−1265. [10d] W. O. Koch, V. Schunemann, M. Gerdan, A. X. Trautwein, H. J. Kruger, *Chem. Eur. J.* **1998**, *4(4)*, 686−691. [10e] H. J. Krüger, *Chem. Ber.* **1995**, *128*, 531−539. [10f] W. O. Koch, H. J. Kruger, *Angew. Chem. Int. Ed. Engl.* **1995**, *34 (23/24)*, 2671−2674.

[11] Samples as prepared required the reported reaction time for full conversion. The different reaction times found for different complexes could reflect differences in reactivity and/or differences in particle size distribution.

[12] O$_\beta$ and C$_\beta$ (O2 and C2) are positioned above and below the O1−M−C1 plane: the displacement of O2 from this plane is +0.51 Å in **8a**A$^+$ and −0.47 Å in **8aB**$^+$, versus +0.49 Å in the

3-platina-1,2-dioxolane **1**. The displacement of C2 is −0.26 Å in **8a**A^+ and +0.29 Å in **8a**B^+, versus −0.29 in the 3-platinadioxolane.

[13] This range is based on O−O distances in 48 crystal structures containing a M−O−O−C fragment (M = any metal); 4 outliers were not taken into account.

[14] This range is based on O−C distances in 48 crystal structures containing a M−O−O−C fragment (M = any metal); 9 outliers were not taken into account.

[15] Bzbpa = *N*-benzyl-*N*,*N*-bis(2-pyridylmethyl)amine.

[16] B. de Bruin, J. A. W. Verhagen, C. H. J. Schouten, A. W. Gal, D. Feichtinger, D. A. Plattner, *Chem. Eur. J.* **2001**, *7(2)*, 416−422.

[17] For some examples see: [17a] J. C. M. Ritter, R. G. Bergman, *J. Am. Chem. Soc.* **1997**, *119*, 2580−2581. [17b] K. J. Del Rossi, X. X. Zhang, B. B. Wayland, *J. Organomet. Chem.* **1995**, *504*, 47−56.

[18] Space group before and after transformation: *C*2/*c*. Cell dimensions before transformation: a = 35.8688(5), b = 10.7328(2), c = 24.2609(4) Å, β = 116.666(1)°, V = 8346.4(2) Å^3. Cell dimensions after transformation: a = 36.0362(2), b = 10.7760(1), c = 24.2975(2) Å, β = 116.3883(4)°, V = 8452.2(2) Å^3 (see Table 5).

[19] A. N. J. Blok, P. H. M. Budzelaar, M. Krom, A. W. Gal, paper to be published.

[20] Yields and reaction times highly depend on the presence of (small amounts of) water and protonation of the counterion, which both influence the acidity of the solution.

[21] [21a] B. R. Flynn, L. Vaska, *J. Am. Chem. Soc.* **1973**, *95(15)*, 5081−5083. [21b] T. Yoshida, D. L. Thorn, T. Okano, J. A. Ibers, S. Otsuka, *J. Am. Chem. Soc.* **1979**, *101(15)*, 4212−4221. [21c] S. F. Hossain, K. M. Nicholas, C. L. Teas, R. E. Davis, *J. Chem. Soc., Chem. Commun.* **1981**, 268−269.

[22] The ESI-MS spectrum also shows a peak at m/z = 467, but since both the ^{1}H NMR and ^{13}C NMR spectra (measured at 233 K) do not show any peaks that could stem from a second product, we have no explanation for the origin of this peak.

[23] See e.g.: [23a] H. Büning, J. Altman, H. Zorbas, W. Beck, *J. Inorg. Biochem.* **1999**, *75(4)*, 269−279. [23b] K. Tajima, S. Oka, T. Edo, S. Miyake, H. Mano, K. Mukai, H. Sakurai, K. Ishizu, *J. Chem. Soc., Chem. Commun.* **1995**, (*15*), 1507−1508. [23c]P. N. Balasubramanian, E. S. Schmidt, T. C. Bruice, *J. Am. Chem. Soc.* **1987**, *109(25)*, 7865−7873.

[24] R. Cramer, *Inorg. Synth.* **1990**, *28*, 86−88.

[25] G. Anderegg, F. Wenk, *Helv. Chim. Acta* **1967**, *50(243)*, 2330−2332.

[26] H. Nagao, N. Komeda, M. Mukaida, M. Suzuki, K. Tanaka, *Inorg. Chem.* **1996**, *35*, 6809−6815.

[27] [27a] F. Bottino, M. De Grazia, P. Finocchario, F. R. Fronczek, A. Mamo, S. Pappalardo, *J. Org. Chem.* **1988**, *53*, 3521−3529. [27b] H. J. Krüger, personal communication.

[28] J. L. Herdé, J. C. Lambert, C. V. Senoff, *Inorg. Synth.* **1974**, *15*, 18−20.

[29] M. Brookhart, B. Grant, A. F. Volpe Jr., *Organometallics* **1992**, *11*, 3920−3922.

[30] P. T. Beurskens, G. Beurskens, M. Strumpel, C. E. Nordman, in: *Patterson and Pattersons* (Eds.: J. P. Glusker, B. K. Patterson, M. Rossi) Clarendon Press, Oxford, **1987**, 356−367.

[31] *DIRDIF-96.* A computer program system for crystal structure determination by Patterson methods and direct methods applied to difference structure factors: P. T. Beurskens, G. Beurskens, W. P. Bosman, R. de Gelder, S. García-Granda, R. O. Gould, R. Israël, J. M. M. Smits, Crystallography Laboratory, University of Nijmegen, The Netherlands, **1996**.

[32] A. L. Spek, *Acta Crystallogr., Sect. A* **1990**, *46*, C-34.

[33] *PLATON-93.* Program for display and analysis of crystal and molecular structures: A. L. Spek, University of Utrecht, The Netherlands, **1995**.

[34] Immersion Lamp TQ 150 of Heraeus Noblelight GmbH; power consumption: 150 W. The experimental setup is available as Supporting Information.

Received July 23, 2002
[I02410]